THE JOURNAL OF BIOLOGICAL CHEMISTRY VOL. 291, NO. 38, pp. 19923–19938, September 16, 2016

Type IV Pilus Alignment Subcomplex Proteins PilN and PilO Form Homo- and Heterodimers *in Vivo*[*]

Received for publication, May 16, 2016, and in revised form, July 28, 2016 Published, JBC Papers in Press, July 29, 2016, DOI 10.1074/jbc.M116.738377

Tiffany L. Leighton[‡], Daniel H. Yong[‡], P. Lynne Howell[§¶1], and Lori L. Burrows[‡2]

From the [‡]Department of Biochemistry and Biomedical Sciences and the Michael G. DeGroote Institute for Infectious Disease Research, McMaster University, Hamilton, Ontario L8S 4K1 and the [§]Program in Molecular Structure and Function, The Hospital for Sick Children and [¶]Department of Biochemistry, University of Toronto, Toronto M5G 0A4 Ontario, Canada

Pseudomonas aeruginosa **is a leading cause of hospital-acquired infections and is resistant to many antibiotics. Type IV pili (T4P) are among the key virulence factors used by *P. aeruginosa* for host cell attachment, biofilm formation, and twitching motility, making this system a promising target for novel therapeutics. Point mutations in the conserved PilMNOP alignment subcomplex were previously shown to have distinct effects on assembly and disassembly of T4P, suggesting that it may function in a dynamic manner. We introduced mutations encoding Cys substitutions into *pilN* and/or *pilO* on the chromosome to maintain normal stoichiometry and expression levels and captured covalent PilNO heterodimers, as well as PilN and PilO homodimers, *in vivo*. Most covalent PilN or PilO homodimers had minimal functional impact in *P. aeruginosa*, suggesting that homodimers are a physiologically relevant state. However, certain covalent homo- or heterodimers eliminated twitching motility, suggesting that specific PilNO configurations are essential for T4P function. These data were verified using soluble N-terminal truncated fragments of PilN and PilO Cys mutants, which purified as a mixture of homo- and heterodimers at volumes consistent with a tetramer. Deletion of genes encoding alignment subcomplex components, PilM or PilP, but not other T4P components, including the motor ATPases PilB or PilT, blocked *in vivo* formation of disulfide-bonded PilNO heterodimers, suggesting that both PilM and PilP influence the heterodimer interface. Combined, our data suggest that T4P function depends on rearrangements at PilN and PilO interfaces.**

Many bacteria, including *Pseudomonas aeruginosa,* use type IV pili (T4P)[3] for surface attachment/adhesion, biofilm formation, and twitching motility (1–6). T4P are divided into T4aP and T4bP subgroups, based on differences in pilin size and organization of the assembly machinery (6, 7). Here we focus on T4aP, henceforth referred to as T4P. T4P are long, thin, fibrous appendages, which extend from the bacteria, attach to a surface, and are retracted back into the cell, winching the cell forward. This flagellum-independent form of locomotion is called twitching motility. Four subcomplexes make up a T4P machine in *P. aeruginosa* as follows: the outer membrane (OM) secretin (PilQ) and its pilotin (PilF) (8–12); the inner membrane (IM) platform protein (PilC) and cytoplasmic motor proteins (ATPases PilBTU) (13, 14); the helical pilus fiber, composed mainly of the major pilin subunit (PilA) plus minor pilins (PilVWXE and FimU) and adhesin PilY1 (5, 15, 16); and the alignment subcomplex proteins (PilMNOP) that span from the cytoplasm to the OM secretin (17–20). PilN and PilO are bitopic IM proteins with similar predicted secondary structures. These proteins are essential for T4P function and connect the cytoplasmic alignment subcomplex component, PilM, with the IM-associated lipoprotein PilP that interacts with the N0 domain of the secretin monomer PilQ (19, 21). Proposed functions of the PilMNOP subcomplex include aligning the IM motor with the OM secretin, concentrating pilin subunits at the site of extension and retraction, and possibly transducing signals via conformational changes from the cytoplasmic ATPases to generate "open" or "closed" states of the gated secretin (19, 20).

The T4P and type II secretion (T2S) systems have analogous components and similar architecture (22, 23). Whereas the T4P system extends and retracts an elongated pilus, the T2S system specializes in secreting protein substrates from the periplasm into the environment, using a short piston-like "pseudopilus" (23–25). Although the systems have different outputs, their underlying functional mechanisms, which remain to be deciphered, are thought to be comparable. Orthologous components of the alignment subcomplexes in the two systems (PilMN/GspL, PilO/GspM, and PilP/GspC) have limited sequence identity, but atomic resolution structures revealed a high degree of structural similarity, and all three components form equimolar complexes with a ratio of 1:1:1 (18, 20, 26–30). PilN- and PilO-like proteins in the T2S system (GspL and GspM, respectively) form both homo- and heterodimers, although it is not yet clear whether the T4P system is similar (26, 27, 31–34). Previous work in *P. aeruginosa* showed that PilP fails to interact with a PilO homodimer and requires both PilN and PilO for stability (17, 20). Although PilO crystallized as a homodimer (18), complementation of a *pilO* mutant with a plasmid-encoded copy of the gene led to formation of predominantly PilO homodimers at the cost of PilN stability, and thus T4P function (17). In *Thermus thermophilus,* purified T4P

* This work was supported by Operating Grant MOP-93585 from the Canadian Institutes of Health Research (to L. L. B. and P. L. H.). The authors declare that they have no conflicts of interest with the contents of this article.

[1] Recipient of a Tier I Canada Research Chair. To whom correspondence may be addressed: 20-9-715 Peter Giligan Centre for Research and Learning, 686 Bay St., Toronto, Ontario M5G 0A4, Canada. Tel.: 416-813-5378; Fax: 416-813-5022; E-mail: howell@sickkids.ca.

[2] To whom correspondence may be addressed: 4H18 Health Sciences Centre, 1200 Main St. West, Hamilton, Ontario L8N 3Z5 Canada. Tel.: 905-525-9140 (Ext. 22029); Fax: 905-522-9033; E-mail: burrowl@mcmaster.ca.

[3] The abbreviations used are: T4P, type IV pili; OM, outer membrane; IM, inner membrane; β-ME, β-mercaptoethanol; T2S, type II secretion; TMS, transmembrane segment; FRT, FLP recombination target; Cb, carbenicillin; Gm, gentamicin.

alignment subcomplex components were estimated by negative stain cryoelectron microscopy to be in a ratio of 2:2:2 for PilM/PilN/PilO, where initial PilN homodimers in complex with PilM were disrupted by the addition of PilO, ultimately forming PilNO heterodimers (29). These observations, coupled with data from the *P. aeruginosa* system, suggested that the PilNO heterodimer was the relevant functional state *in vivo*, whereas PilN and PilO homodimers might represent intermediates during formation of the assembly system or in complementation experiments, artifacts of overexpression (20).

Cysteine disulfide-bonding analysis is useful for clarifying protein tertiary and quaternary structure and for investigating dynamic interactions among components of cellular machineries (35, 36). The ability of two Cys residues to form a disulfide bond depends on the proximity of their side chains, with bond formation occurring in an oxidizing environment at a Cβ-Cβ distance of 4–8 Å (37). Disulfide bonding imposes structural constraints, and analysis of its effects on function can reveal the importance of conformational changes. Using Cys substitution mutants, *in vivo* formation of both homo- and heterodimers of GspL and GspM was reported for the T2S system of *Dickeya dadantii* (34). The authors suggested that alternative interactions between homo- and heterodimers of GspL and GspM, *i.e.* GspLL and GspMM *versus* two of GspLM, occurred *in vivo*. Formation of disulfide bonds between residues that were predicted to be outwardly facing suggested that these interactions might be controlled through rotation of the proteins, including their transmembrane segments (TMSs) (34). This mechanism was proposed to propagate movement from the cytoplasmic to periplasmic regions of the T2S system machinery, when the ATPase GspE, equivalent to T4P extension ATPase PilB, interacted with the cytoplasmic domain of GspL, equivalent to PilM (34). The interaction itself, or the hydrolysis of ATP and resulting conformational changes in GspE, could induce a corresponding change in GspL, transduced to GspM through their interaction. Previous work in the T2S system and, more recently, the T4P system provided evidence for interactions between the equivalents of PilM and the cytoplasmic ATPase, PilB, either directly or in conjunction with the platform protein PilC (38–41). These interactions might similarly transduce conformational changes that contribute to pilus assembly or disassembly.

We hypothesized that dynamic movement of the T4P alignment subcomplex proteins PilN and PilO may occur during (or because of) extension and retraction of pili and that PilO's ability to interact with both itself and PilN may reflect a functionally relevant switch between homo- and heterodimers. To test this idea, we introduced Cys substitutions at predicted interfaces between PilNO and PilOO, and we used non-reducing SDS-PAGE to observe dimer formation. Covalent PilN and PilO homodimers, as well as PilNO heterodimers, were captured *in vivo* under physiological conditions. Depending on the location, disulfide bonding disrupted the normal function of the T4P system, inhibiting motility. Deletion of the motor ATPases had no effect on the dimerization state of PilN and PilO, arguing against a link between motor function and conformational switching, but loss of either PilM or PilP specifically blocked PilNO heterodimer formation. These data provide new insights into the architecture and dynamics of the T4P system.

Results

Selection of Residues for Cys Substitution—Our PilO homodimer structure (Protein Data Bank code 2RJZ) (18) was used to identify candidate residues predicted to be within appropriate distances for disulfide bond formation (Fig. 1*A, top*). In the PilO model, two relevant interfaces were identified as follows: the core, comprising mainly contacts between the α4-helix and β4-strand; and the coiled coils, between the α1- and α2-helices (18). In the $PilO_{\Delta 68}$ model, the coiled-coils are truncated and folded back, because they are not anchored in the IM. Because of the potentially artificial nature of that particular interaction interface, we focused on residues in the core region previously shown to be important for function (42). Residues in the α4-helix and β4-strand of the PilO homodimer model with an estimated distance between β-carbons of less than 8 Å were selected for mutagenesis (Fig. 1*A*, *bottom*) (37, 43, 44).

All attempts to purify soluble *P. aeruginosa* PilN for structural studies, or to solve an x-ray crystal structure of the PilNO heterodimer, have so far been unsuccessful. The structure of a periplasmic portion of PilN from *T. thermophilus* is available (29); however, due to the low primary sequence identity with PilN from *P. aeruginosa*, as well as a different arrangement of secondary structure elements (*Thermus* PilN has an extra α-helix inserted in the first $\alpha\beta\beta$ motif), we were unable to generate a high confidence model using that structural template. *P. aeruginosa* PilN is predicted to have a structural organization similar to PilO, and thus we used the truncated *P. aeruginosa* PilO homodimer structure (18) to generate a high confidence Phyre[2] (45) model of a $PilN_{\Delta 57}$ monomer, and we used the PilO homodimer interface to model a PilNO heterodimer using the same core-core interface (Fig. 1*B, top*) (42). This model was used to design a series of single Cys substitutions in the α4-helix and β4-strand of either PilN or PilO (Fig. 1*B, bottom*). The PilNO model has been partially validated in previous work (42), but for this study, we included a negative control Cys pair ($PilN^{R142C}$/$PilO^{A158C}$) at a Cβ distance of over 12 Å, considered too far for disulfide bond formation (37, 44).

To avoid issues arising from non-stoichiometric expression, the mutations encoding the Cys substitutions of interest were introduced at the native *pilMNOPQ* locus of *P. aeruginosa* PAK by homologous recombination. Screening of the sequence-verified mutants for effects on expression and stability of each of the inner membrane alignment subcomplex proteins revealed no effects of the Cys substitutions on PilMNOP levels relative to wild type (Fig. 2*A*).

Formation of Cys Cross-linked PilNO and PilOO Dimers in Vivo—Whole cell lysates of all mutants were analyzed in parallel in reducing and non-reducing conditions, followed by immunoblotting with anti-PilN or PilO antibodies. Of the PilNO Cys substitutions, only the $PilN^{R142C}$/$PilO^{D175C}$ variant formed significant levels of cross-linked dimers *in vivo* (Fig. 2, *B* and *C*). Two bands appeared on the anti-PilN blot (Fig. 2*B*), at the sizes consistent with *in vivo* formation of a PilNO heterodimer (44.7 kDa) and, unexpectedly, a PilN homodimer (43.8 kDa). Of the PilO double Cys mutants, both $PilO^{A158C/I178C}$ and

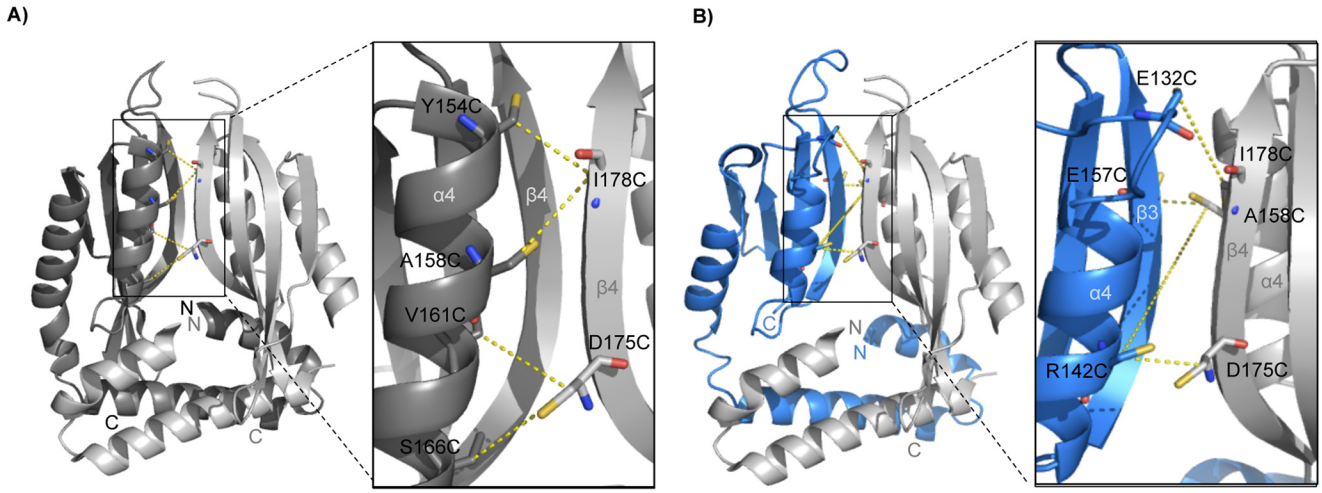

PilO (α4 helix)	PilO (β4 strand)	Distance (Å)
S166C	D175C	4.9
V161C	D175C	6.3
A158C	I178C	6.6
Y154C	I178C	7.2

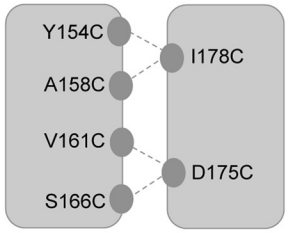

PilN (blue)	PilO (grey)	Distance (Å)
R142C	D175C	5.1
E157C	A158C	3.8
E132C	I178C	7.7
R142C	A158C	18.7

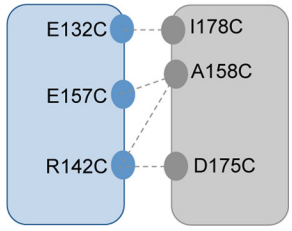

FIGURE 1. **Locations of residues chosen for Cys substitution mutagenesis in PilN and PilO.** A schematic diagram representation mapping the N and C termini, secondary structure elements, and structural domains of a $PilO_{\Delta 68}$ dimer (2RJZ (18)) (*A*) or a $PilN_{\Delta 57}$ (*blue*) and $PilO_{\Delta 68}$ (*gray*) heterodimer using a Phyre[2] model (45) (*B*) of PilN generated using the $PilO_{\Delta 68}$ homodimer as template. The core-core domains consist of PilN α-helices 3–4 and β-strands 1–4 and PilO α-helices 3–4 and β-strands 1–5. *Inset* shows zoomed view of interaction interface with residue substitutions labeled accordingly. *Bottom*, *tables* indicate the distance between the Cβ of the substituted Cys residues (in angstroms) and schematic depiction of residue locations.

$PilO^{Y154C/I178C}$ variants formed cross-linked dimers *in vivo* (Fig. 2*C*) at a size consistent with that of PilO homodimers (45.6 kDa). Thus, at least one of each set of selected residue pairs formed the predicted linkage (Fig. 2*D*). This is the first evidence in any T4P system for PilN homodimerization under physiological conditions.

To further investigate PilN homodimerization, we leveraged a previously described $PilN_{\Delta 44}/PilO_{\Delta 51\_His}$ co-expression construct (20) that encodes truncated forms of both proteins. These proteins lack their short cytoplasmic N termini and transmembrane segments and encompass a larger portion of the periplasmic domains than the construct used to obtain the aforementioned $PilO_{\Delta 68}$ homodimer structure. A PilN Cys mutant ($PilN_{\Delta 44}{}^{R142C}/PilO_{\Delta 51}$), a PilO Cys mutant ($PilN_{\Delta 44}/PilO_{\Delta 51}{}^{D175C}$), or a double PilNO Cys pair ($PilN_{\Delta 44}{}^{R142C}/PilO_{\Delta 51}{}^{D175C}$) were expressed in *E. coli* Origami 2 DE3, which has a non-reducing cytoplasm to allow for the formation of disulfide bonds, and purified using nickel-nitrilotriacetic acid affinity chromatography. Purified proteins were separated under reducing or non-reducing conditions and probed with anti-PilN and PilO antibodies. The $PilN_{\Delta 44}{}^{R142C}/PilO_{\Delta 51}$ pair yielded disulfide-bonded PilN homodimers (~34.0 kDa) (Fig. 3*A*). Interestingly, the same proteins also formed apparent PilNO heterodimers, as PilN monomers were still visible in the non-reducing lane. Because PilN is unstable/insoluble in the absence of PilO (20), this result suggests that a proportion of PilN monomers did not participate in covalent self-interactions but rather in non-covalent interactions with PilO. For $PilN_{\Delta 44}/PilO_{\Delta 51}{}^{D175C}$, PilO homodimers (~36.4 kDa) were clearly visible in the anti-PilO blot, showing that PilO occupies both homo- and heterodimer states (Fig. 3*B*). When both PilN and PilO contained Cys substitutions ($PilN_{\Delta 44}{}^{R142C}/PilO_{\Delta 51}{}^{D175C}$), three subpopulations were identified as follows: PilN homodimers, PilO homodimers, and PilNO heterodimers (~35.2 kDa; Fig. 3, *A* and *B*). In this case, nearly all PilN monomers were involved in covalent interactions in non-reducing conditions (Fig. 3, *A* and *B*) when compared with PilO. This suggests that PilO homodimers might occupy multiple orientations, some disulfide-bonded and others not, implying in the latter case that the $PilO^{D175C}$ mutation was too far or incorrectly oriented for disulfide bond formation. These data confirm the observation that PilN and PilO form homodimers and heterodimers under physiological conditions in *P. aeruginosa*.

Because the untagged covalently linked $PilN^{R142C}$ homodimers purified with C-terminally His-tagged PilO, we realized that PilN homodimers must interact with PilO homodimers via an interface other than the one shown in Fig. 1*B*; the most likely candidate for a second interface was the coiled coils, below the core domains. Using size exclusion chromatography, we confirmed that $PilN_{\Delta 44}{}^{R142C}/PilO_{\Delta 51\_His}$ (as well as unmodified $PilN_{\Delta 44}/PilO_{\Delta 51\_His}$ and other Cys mutants) eluted from an S75 size exclusion column at a volume similar to the conalbumin standard (~75 kDa) (Fig. 3*C*), consistent with a PilNO tetramer (70.4 kDa). Thus, PilNO can simultaneously form homo- and heterodimers via two distinct interfaces.

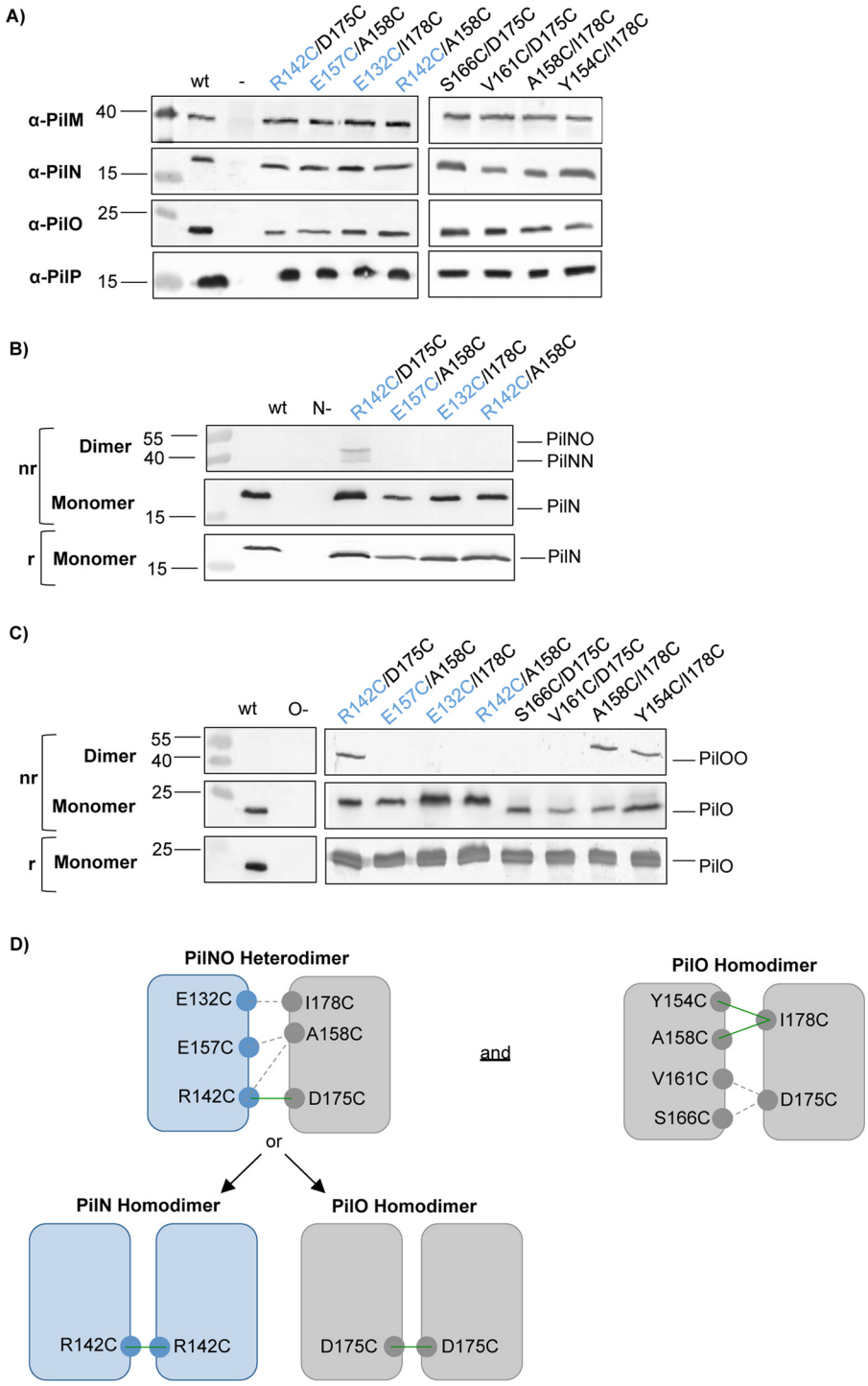

FIGURE 2. **Formation of disulfide-bonded homo- and heterodimers *in vivo*.** Lysates for the wild-type (*wt*), negative controls (−), and the Cys mutants were subject to SDS-PAGE under non-reducing (*nr*) and reducing (*r*) conditions and then blotted with specific antibodies to each alignment subcomplex component (α-PilM, α-PilN, α-PilO, and α-PilP) to confirm stability of each protein in the Cys mutants (*A*), PilN (*B*), and PilO (*C*). $PilN^{R142C}$/$PilO^{D175C}$ was able to form PilNO heterodimers (44.7 kDa) and PilN homodimers (43.8 kDa), whereas $PilO^{A158C/I178C}$ and $PilO^{Y154C/I178C}$ mutants were able to form disulfide bonds and form PilO homodimers (45.6 kDa) *in vivo*. Images are representative of at least three independent experiments. *D,* schematic of the residues that were able to form disulfide bonds (*green lines*) in the cross-linking experiments and their relative locations. *Dashed lines* indicate no dimer formation was observed. The $PilN^{R142C}$/$PilO^{D175C}$ Cys mutants formed PilNO heterodimers but also $PilN^{R142C}$ and $PilO^{D175C}$ homodimers. PilN residues are indicated in *blue text*.

Disulfide Bond Formation between PilN and/or PilO Can Disrupt T4P Function—To assess the functional consequences arising from formation of covalently linked dimers *in vivo*, the ability of the Cys mutant strains to assemble surface-exposed T4P was assessed (Fig. 4*A*). The $PilN^{R142C}$/$PilO^{D175C}$ and $PilO^{A158C/I178C}$ mutants had very low levels of surface pili, and piliation of the $PilO^{Y154C/I178C}$ mutant was comparable with negative controls. Both the $PilO^{S166C/D175C}$ and $PilO^{V161C/D175C}$ mutants had a moderate reduction in surface pili, possibly related to their shared D175C mutation.

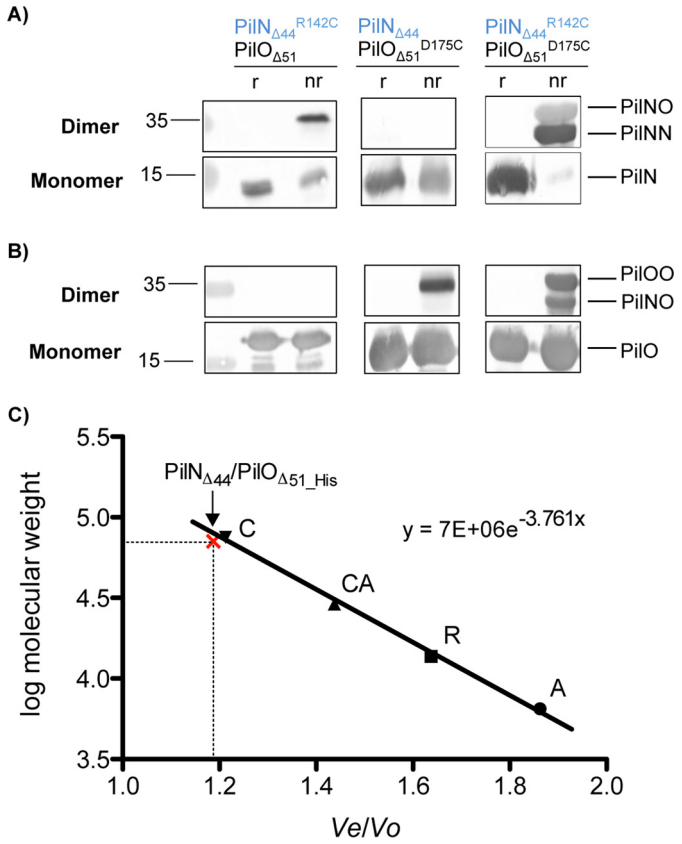

FIGURE 3. **Purification of PilN and PilO tetramers.** PilN$_{\Delta44}$ and PilO$_{\Delta51}$ were co-expressed with either PilN^{R142C}, PilO^{D175C}, or both the PilN^{R142C}/PilO^{D175C} Cys mutations. After nickel affinity purification, the proteins were subject to SDS-PAGE under either non-reducing (*nr*) or reducing (*r*) conditions and blotted with antisera specific for PilN (*A*) or PilO (*B*). We observed the following three disulfide-bonded subpopulations: PilN homodimers (34.0 kDa) in both the PilN^{R142C} and PilN^{R142C}/PilO^{D175C} samples (*left* and *right panels*); PilO homodimers (36.4 kDa) in both the PilO^{D175C} and PilN^{R142C}/PilO^{D175C} samples (*center* and *right panels*); and PilNO heterodimers (35.2 kDa) in the double Cys mutant as well (*right*). *C*, gel filtration calibration curve for the protein standards on a Superdex 75 10/300 GL column; aprotinin (A; 6.5 kDa), RNase A (*R*; 13.7 kDa), carbonic anhydrase (*CA*; 29.0 kDa), and conalbumin (*C*; 75.0 kDa). PilN$_{\Delta44}$ and PilO$_{\Delta51}$ co-eluted at a volume similar to conalbumin as indicated on graph with the *red x* The elution volumes (V_e) of the standards are divided by the void volume of the column (V_0) and plotted against the log of the standards' molecular weights to give the slope of the line that was used to solve for the molecular weight of the eluted PilN$_{\Delta44}$/PilO$_{\Delta51_His}$ complex (70.4 kDa). PilN residues indicated in *blue text*.

These data suggest that pilus biogenesis requires specific PilN and PilO configurations that are perturbed by these mutations.

Because T4P function relies on the dynamic assembly and disassembly of pili, it was important to assess motility as well as piliation levels (Fig. 4*B*). Strains forming covalently cross-linked dimers (PilN^{R142C}/PilO^{D175C}, PilO$^{A158C/I178C}$, and PilO$^{Y154C/I178C}$) were incapable of twitching. PilO$^{S166C/D175C}$ and PilO$^{V161C/D175C}$ strains had approximately half of wild-type motility, consistent with their decrease in piliation levels, although no *in vivo* cross-linked dimers were observed for these mutants. The remaining Cys mutants twitched similarly to the wild type.

Lack of Piliation Is Caused by Inefficient Assembly—Any pili assembled in strains lacking the retraction ATPase, PilT, become trapped on the cell surface (46). Loss of pilus retraction in alignment subcomplex mutants was shown previously (14) to allow for capture of a few pili on the surface of the cells. Because three of the double Cys mutants had reductions in the levels of surface pili (PilN^{R142C}/PilO^{D175C}, PilO$^{A158C/I178C}$, and PilO$^{Y154C/I178C}$), we hypothesized that they would assemble more pili in a retraction-deficient background, similar to *pilN* or *pilO* mutants. We disrupted *pilT* in these backgrounds and tested the resulting levels of surface piliation. As predicted, all mutants assembled more pili when retraction was disabled (Fig. 4*C*). This result suggests that all mutants are capable of extending pili but that assembly in those backgrounds is inefficient, especially in the PilO$^{Y154C/I178C}$ mutant, resulting in net pilus retraction when PilT is active.

Specific Single Cys Mutations Affect Function of the T4P System—Because moderate reductions in twitching and piliation were observed in two PilO double Cys mutant strains that share a common substitution (PilO$^{S166C/D175C}$ and PilO$^{V161C/D175C}$), we next investigated whether individual Cys substitutions disrupted T4P production and/or function. The stability of alignment subcomplex components in strains with single Cys substitutions was tested using specific antibodies, and the levels of PilMNOP were found to be comparable with wild type (Fig. 5*A*). Each single Cys mutant produced pili at levels similar to wild type, with the exception of PilN^{R142C} that had a modest reduction in piliation (Fig. 5*B*). Interestingly, neither PilN^{R142C} nor PilO^{D175C} could twitch (Fig. 5*C*), even though both produced pili; this phenotype is a hallmark of retraction defects. When the retraction ATPase PilT was deleted from PilN^{R142C} and PilO^{D175C}, their piliation levels were similar to the *pilT* control, showing they are capable of wild-type pilus assembly (Fig. 5*D*). Motility, and therefore pilus retraction, of all other single Cys mutants was unaffected.

Single Cys Substitutions Allow for in Vivo Homodimer Formation, but Only a Subset Has Functional Consequences—To better understand why PilN^{R142C} and PilO^{D175C} single mutants could extend pili but not twitch, we hypothesized that these substitutions might trap PilN or PilO in specific homodimer configurations, impairing function. Whole cell lysates of all single Cys mutants were analyzed in reducing and non-reducing conditions followed by immunoblotting with PilN and PilO antibodies. We were surprised to see that all single Cys mutants formed covalent homodimers *in vivo* to varying degrees, with PilN^{R142C} and PilO^{Y154C} forming the most, and fewer dimers captured for other Cys mutants such as PilO^{D175C} and PilO^{V161C}, where dimer formation is harder to detect (Fig. 5, *E* and *F*). These data suggest that with specific exceptions (PilN^{R142C} and PilO^{D175C}), covalent *in vivo* homodimerization of PilN and PilO can occur without functional consequences.

Heterodimer Formation of PilN^{R142C} and PilO^{D175C} Is Abolished in a pilM Background—As proposed for the T2S system (34), partner switching, or reorientation of PilN and PilO interfaces, might explain how PilN and PilO can form both homo- and heterodimers *in vivo*. We hypothesized that PilN might respond to conformational changes in its cytoplasmic partner PilM, repositioning it relative to PilO. To test whether formation of covalent dimers requires PilM, the *pilM* gene was deleted in each of the PilN^{R142C}/PilO^{D175C}, PilO$^{A158C/I178C}$, and PilO$^{Y154C/I178C}$ strains. The absence of PilM was confirmed by Western blot (Fig. 6*A*), and whole cell lysates of Cys mutant strains lacking PilM were analyzed in reducing

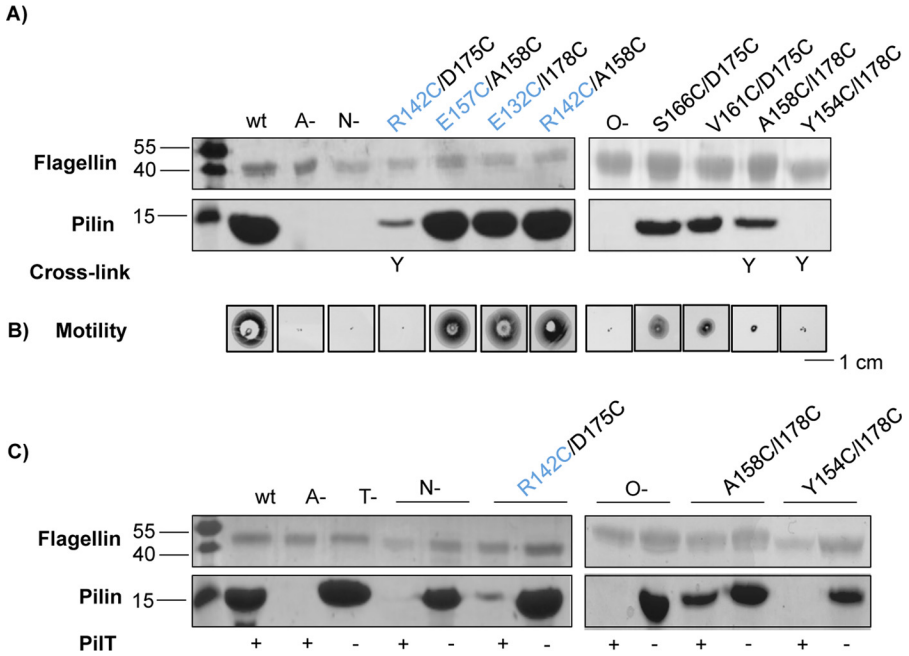

FIGURE 4. **Functional consequences of covalent dimer formation in wild type and retraction-deficient backgrounds.** PilN and PilO Cys mutants, plus wild type (*wt*), non-piliated (*A*−), hyperpiliated (*T*−), and negative controls (*N-* and *O-*) were tested for sheared surface pili (*A*), and twitching motility (*B*). Sheared surface preparations revealed that the PilN^{R142C}/PilO^{D175C} and PilO$^{A158C/I178C}$ mutants exhibited severely reduced levels of surface pili, although the PilO$^{Y154C/I178C}$ mutant exhibited no surface-exposed pili, and all were devoid of twitching motility similar to negative controls. Large disruptions in motility and piliation in the remaining PilNO Cys pairs were not observed. The ability of PilNO or PilOO Cys pairs to form Cys cross-links is indicated below (*Y*). *C,* select Cys mutants were introduced into a retraction-deficient background, which revealed that all three double Cys mutants assemble more pili without the retraction ATPase, PilT. PilT presence (+) or absence (−) in each strain is indicated below. Images are representative of at least three independent experiments.

and non-reducing conditions, followed by immunoblot analysis with PilN or PilO antibodies. Although both PilO$^{A158C/I178C}$ and PilO$^{Y154C/I178C}$ formed covalent homodimers in the absence of PilM, PilN^{R142C}/PilO^{D175C} no longer formed covalent heterodimers (Fig. 6, *B* and *C*).

Heterodimer Formation by PilN^{R142C} and PilO^{D175C} Is Also Abolished in a pilP Background—To determine whether the remaining member of the alignment subcomplex, PilP, had effects on PilNO dimer formation, we created a *pilP* strain expressing the Cys pairs of interest (PilN^{R142C}/PilO^{D175C}, PilO$^{A158C/I178C}$, and PilO$^{Y154C/I178C}$), confirmed loss of PilP by Western blot (Fig. 6*A*), and analyzed whole cell lysates as described above. The PilN^{R142C}/PilO^{D175C} strain failed to form covalent PilNO heterodimers in the absence of PilP; however, PilN and PilO formed homodimers (Fig. 6, *D* and *E*), as in the *pilM* mutant. To investigate whether the absence of PilP alone affected the PilNO interface, or whether the change in dimerization state was due to the lack of PilNO tethering via PilP to the N0 domain of PilQ (19), we created a *pilQ* strain expressing the PilN^{R142C}/PilO^{D175C} Cys pair, confirmed loss of PilQ by Western blot (Fig. 6*A*), and tested lysates as described above. Absence of PilQ had no effect on homo- or heterodimer formation (Fig. 6, *F* and *G*), suggesting that PilP specifically contributes to the formation of an interface conducive to the formation of a covalent bond between PilN^{R142C}/PilO^{D175C}.

Other T4P Components Do Not Modulate the PilNO Interface—Recently, interactions between PilM and motor ATPases of the T4P system were identified for both *P. aeruginosa* and *M. xanthus* (40, 41). Because PilM was important for formation of covalent PilN^{R142C}/PilO^{D175C} heterodimers, we hypothesized that conformational changes in PilM, driven by its interaction with other cytoplasmic components of the T4P motor while bound to the N terminus of PilN, might be propagated to and affect the orientation of periplasmic PilNO interfaces. Three AAA^{+}-ATPases modulate extension (PilB) and retraction (PilTU) of the pilus fiber (5, 47, 48). We created *pilB*, *pilT*, and *pilU* mutants containing the Cys pairs of interest (PilN^{R142C}/PilO^{D175C}, PilO$^{A158C/I178C}$, and PilO$^{Y154C/I178C}$) and confirmed the absence of each ATPase by Western blotting (Fig. 7). Unexpectedly, all strains formed covalent homo- and heterodimers (Fig. 8, *B*, *D*, and *E*), suggesting that the ATPases do not influence the PilNO interface.

We further investigated whether other T4P components associated with PilM, PilN, or PilO, including PilA, the major component of the pilus fiber and PilC, the IM platform protein, influenced the dimerization state of PilN and PilO. Strains with disruptions in *pilA* or *pilC,* plus the above Cys substitutions (Fig. 7), formed covalent homo- and heterodimers similar to the wild type (Fig. 8, *A* and *C*). These data suggest that only interactions among members of the alignment subcomplex modulate the interface between PilN and PilO.

Discussion

The PilMNOP alignment subcomplex is highly conserved among T4aP-expressing bacteria (5). Previous studies demonstrated that PilN and PilO form stable heterodimers in a 1:1 stoichiometry (18); however, the precise interface(s) between PilN and PilO has not yet been elucidated. We used disulfide-bonding analysis to study the interactions between these components and to assess the functional consequences of covalently cross-linking PilN and/or PilO. Our results revealed that PilN and PilO form both homo- and heterodimers *in vivo* under

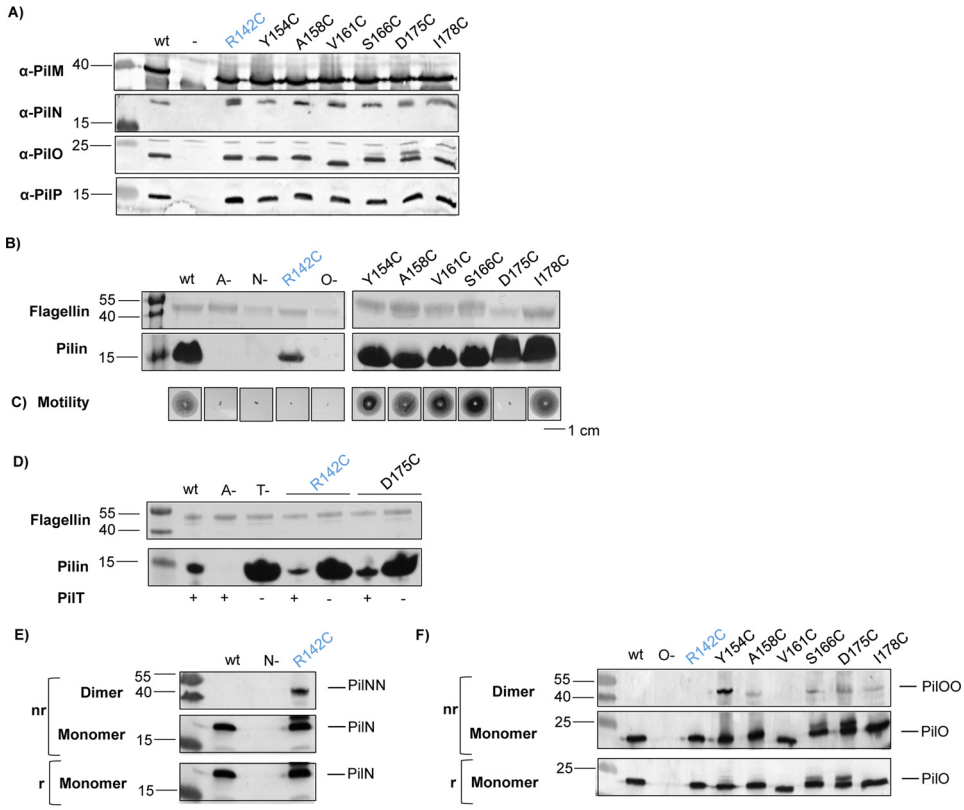

FIGURE 5. **PilN^{R142C} and PilO^{D175C} single Cys substitutions cause T4P dysfunction in wild-type and retraction-deficient backgrounds.** Lysates for the wild type (*wt*), negative controls (−), and the Cys mutants were subject to SDS-PAGE and then blotted with specific antibodies to each alignment subcomplex component (α-PilM, α-PilN, α-PilO, and α-PilP) to confirm stability of each protein in the Cys mutants (*A*). Each mutant along with wild type, non-piliated (*A*−), hyperpiliated (*T*−), and negative controls (*N*- and *O*-) were tested for sheared surface pili (*B*), and twitching motility (*C*). PilN^{R142C} had less pili and motility than WT, whereas PilO^{D175C} had similar level of pili but no motility. *D*, PilN^{R142C} and PilO^{D175C} were introduced into a retraction-deficient background, which revealed that both Cys mutants can assemble more pili without the retraction ATPase, PilT. PilT presence (+) or absence (−) in each strain is indicated below. Whole cell lysates were then subjected to SDS-PAGE under non-reducing (*nr*) and reducing (*r*) conditions and then blotted with specific antibodies to PilN (*E*), and PilO (*F*). All single Cys mutants formed homodimers to varying extents. Images are representative of at least three independent experiments.

physiological conditions and that conformational flexibility of these states is necessary for T4P function.

PilN and PilO May Form Functional Dimers of Dimers in Vivo—Studies in the T2S system showed that PilN- and PilO-like proteins (GspL and GspM, respectively) form homo- and heterodimers, possibly via a process called "partner switching," implying large rotations in the TMS and core interfaces (34). Here, we captured PilO homodimers, previously observed only upon overexpression in *trans* (17, 18), when expressed at native levels and stoichiometry from the *Pseudomonas* chromosome, confirming that the PilO homodimer interface revealed by structural studies is physiological (Fig. 2*C*). Unexpectedly, while trying to understand whether PilNO heterodimers share the same interface as PilO homodimers, we identified multiple species on an anti-PilN Western blot (Fig. 2*B*), with masses corresponding to PilNO heterodimers and PilN homodimers. Although a PilN homodimer (bound to PilM) from the T4P system of *T. thermophilus* was observed *in vitro* (29), to our knowledge this is the first report of PilN and PilO homodimers in their native context.

When Cys-substituted soluble periplasmic fragments of PilN or PilO (PilN^{R142C} and PilO^{D175C}, Fig. 3, *A* and *B*) were expressed in *E. coli*, they formed covalent homodimers. Co-expression of PilO^{D175C} with PilN^{R142C} led to capture of three subpopulations: PilN^{R142C} homodimers, PilO^{D175C} homodimers, and PilN^{R142C}/PilO^{D175C} heterodimers (Fig. 3, *A* and *B*), suggesting that there are (at least) two possible interfaces for each protein. Interestingly, a large amount of PilO monomers remained in the non-reducing lanes, indicating that a substantial proportion of PilO was either present as a monomer or participating in non-covalent dimers, possibly as a result of non-permissive positioning of a PilO interaction interface for disulfide bond formation.

P. aeruginosa PilN expressed *in vitro* without PilO is mostly insoluble (20), which has precluded studies of PilN alone. We hypothesized that formation of covalent PilN homodimers might stabilize it in the absence of PilO, and we attempted to purify PilN$_{\Delta 44_His}^{R142C}$ under non-reducing conditions, but the protein remained mostly insoluble. However, untagged PilN^{R142C} homodimers co-purified with tagged PilO, and the molecular mass of the complex was ~75 kDa (Fig. 3*C*), likely corresponding to a 2:2 PilN$_{\Delta 44}$/PilO$_{\Delta 51_His}$ complex. This stoichiometry is consistent with our previous data, where PilNOP were shown by gel filtration to elute as either a trimer or a dimer of trimers (20). A dimeric complex of PilMNO (2:2:2) was reported for *T. thermophilus* (29), fitting with the idea that *P. aeruginosa* PilN and PilO form a dimer of dimers (17, 19, 20, 29).

Only two of four predicted PilO Cys mutant pairs, and one of three PilNO pairs, formed disulfide bonds, suggesting that the

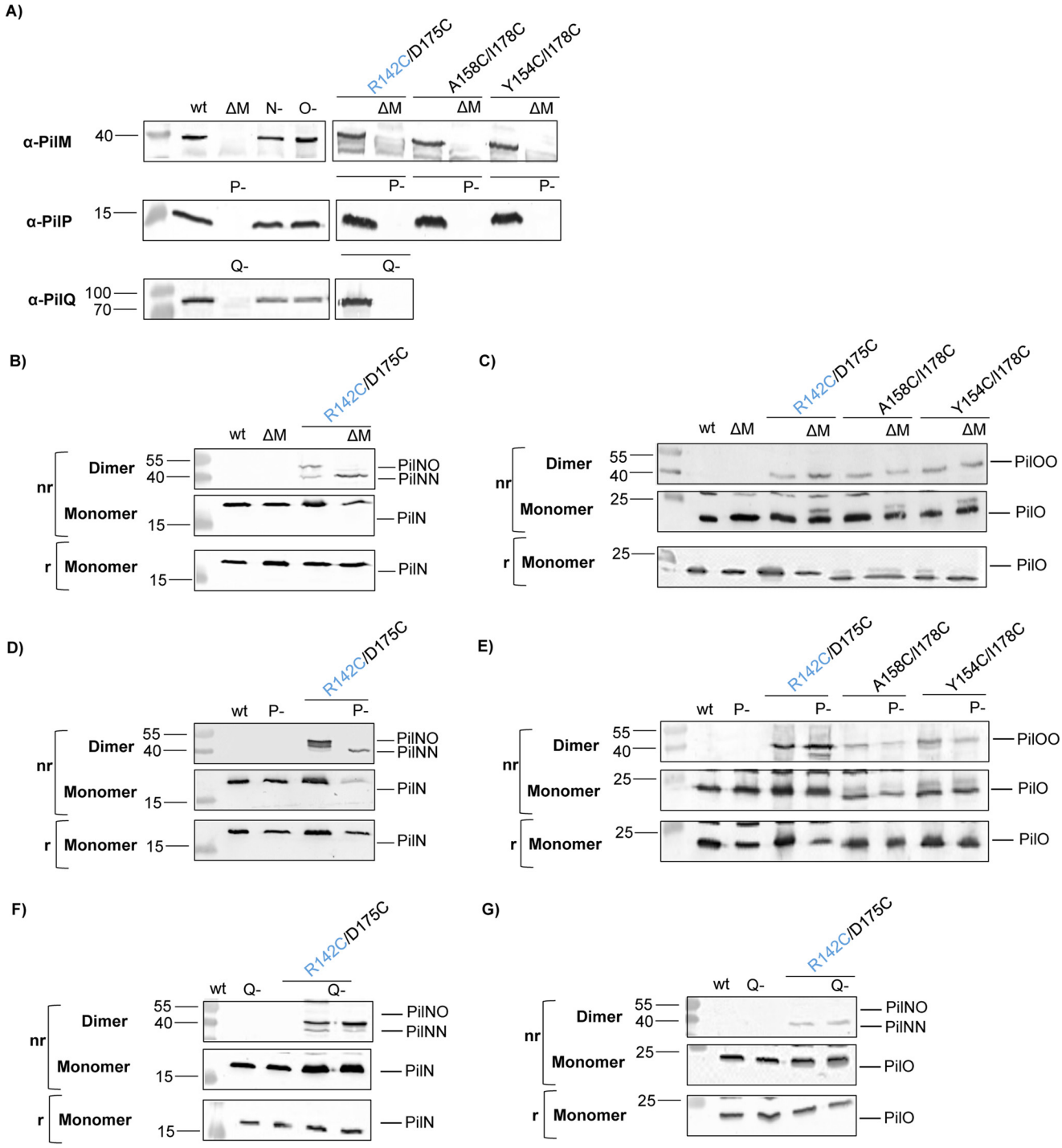

FIGURE 6. **Heterodimer formation is abolished in *pilM* or *pilP* backgrounds.** Lysates of PilN and PilO Cys mutants, wild type (*wt*), PilM deletion (Δ*M*), PilP::FRT (*P-*), and the negative controls (*N-* and *O-*) were resolved using SDS-PAGE under non-reducing (*nr*) and reducing (*r*) conditions and subjected to Western blot detection using specific antibodies to PilM, PilP, and PilQ to show the loss of the proteins (*A*), PilN (*B, D,* and *F*), and PilO (*C, E,* and *G*). Images are representative of at least three independent experiments. In the absence of PilM or PilP, Cys cross-linked homodimers ($PilO^{A158C/I178C}$ and $PilO^{Y154C/I178C}$) still form, whereas the $PilN^{R142C}$/$PilO^{D175C}$ heterodimer cannot. The absence of PilQ does not alter the dimerization profile of the $PilN^{R142C}$/$PilO^{D175C}$ Cys pair.

truncated $PilO_{\Delta 68}$ structure (Fig. 1*A*) (18) and the $PilN_{\Delta 57}$/$PilO_{\Delta 68}$ heterodimer homology model derived from it (Fig. 1*B*) do not exactly mirror the *in vivo* conformation of the proteins. However, the ability to cross-link both homo- and heterodimers of PilN and PilO *in vivo* confirms that select residues are close enough and in the appropriate orientation to allow for disulfide bond formation. The recent cryoelectron tomography study of the *M. xanthus* T4P system (49), with resolutions averaging 4 nm, now offers the exciting possibility that we could use similar approaches to image the T4P systems of our *P. aeruginosa* Cys mutants *in situ*, to visualize how cross-linking of PilNO affects the configuration of the machinery.

Interestingly, the relative position of the Cys residue pairs able to cross-link PilO homodimers *in vivo* were at the "top" of

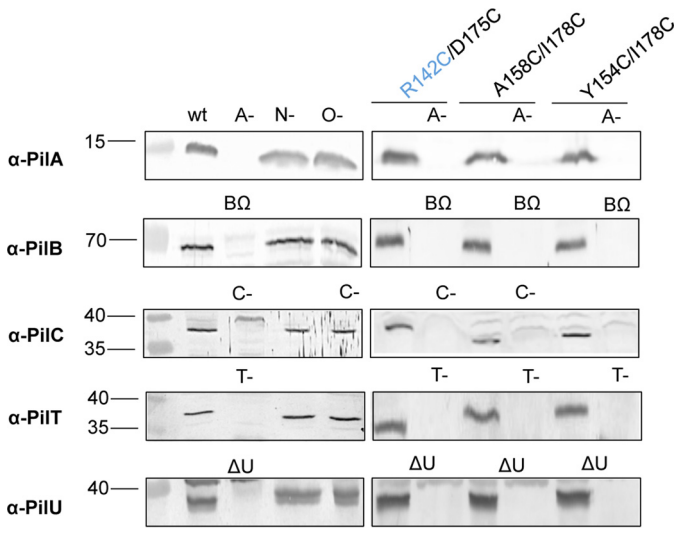

FIGURE 7. **Disruption of *pilA, pilB, pilC, pilT,* and *pilU* in PilN^{R142C}/PilO^{D175C}, PilO$^{A158C/I178C}$, and PilO$^{Y154C/I178C}$ backgrounds.** Lysates of wild type (*wt*), negative control strains (*A-, BΩ, C-, N-, O-, T-,* and *ΔU*), and Cys mutants were tested for expression and stability of each protein using protein-specific antisera. *Minus signs* indicate the gene was disrupted via an FRT insertion; Δ indicates the gene was produced by a deletion of the gene; and Ω indicates the gene was disrupted by an Ω cassette insertion.

the predicted interface in most cases, although they were at the "bottom" for the PilNO heterodimer (Fig. 2*D*), suggesting that the homo- and heterodimer interfaces might be angled differently. Models of the core interaction interface between PilN and PilO in *T. thermophilus* (29) and *M. xanthus* (49) show them as tilted, possibly because of longer predicted coiled coils in PilO (18). The persistence of PilN and PilO monomers (Figs. 2, *B* and *C,* and 3, *A* and *B*) not involved in covalent interactions suggests the co-existence of multiple PilN and PilO interaction species. This scenario was reported for type II secretion system PilP- and PilQ-like proteins (GspC and GspD, respectively), where contacts were established at three distinct interfaces *in vivo* (50). These observations, combined with our results, suggest that homo- and heterodimers may occur simultaneously. Based on these new data, we propose that the oppositely charged coiled coils of PilNO (18) could serve as the primary interaction interface between heterodimers (Fig. 9*B*), whereas the core regions could mediate homodimer interactions (Fig. 9*C*). This revised model better explains our previous findings, where up to six combined point mutations along the PilN core (now proposed to be the homodimer interface) failed to disrupt PilNO heterodimers in a bacterial two-hybrid assay (42). Furthermore, this new model could explain why PilN^{R142C} and PilO^{D75C} residues at the bottom of the original model (Fig. 1) adjacent to the coiled coils participate in both homo- and heterodimers (Figs. 2, *B* and *C,* and 3, *A* and *B*). A tilted PilNO core interface could position these residues in close enough proximity to form a disulfide bond with either partner. Importantly, our data do not support the proposal of large rotations in the core-core interfaces, as suggested previously for the T2S system (34).

PilN and PilO Homodimers May Represent a Functional Rather Than Assembly Intermediate State of the T4P System—Our data show that covalent PilN or PilO homodimers are not necessarily detrimental to function. With the exception of PilN^{R142C} and PilO^{D175C}, both of which assembled pili but had retraction defects that abrogated motility, none of the single Cys mutants had obvious piliation or motility defects (Fig. 5, *B* and *C*), despite their capacity to form covalent homodimers *in vivo* (Fig. 5, *E* and *F*). The relative abundance of covalent homodimers formed by each mutant did not correlate with T4P dysfunction, as PilO^{Y154C} formed the most dimers, but without functional consequences. This result suggests that cross-linking of only specific residues affects function and supports the idea that PilN and PilO homodimers represent a normal functional state of the T4P system.

Three covalent pairs (PilN^{R142C}/PilO^{D175C}, PilO$^{A158C/I178C}$, and PilO$^{Y154C/I178C}$) caused significant loss of surface piliation and complete loss of motility (Fig. 4, *A* and *B*). This result suggests that some configurations of PilNO can affect pilus function. In a retraction-deficient background, where assembled pili are trapped on the surface (46), all three double Cys mutants had more pili (Fig. 4*C*), confirming that covalently linked dimers permit pilus assembly. Thus, lack of motility in these strains more likely arises from extension-retraction imbalances. We showed previously (42) that substitution of specific residues at the coiled-coil interface of PilN and PilO also confers an assembly-competent yet motility-deficient phenotype. Together, these data emphasize that PilNO contribute to both pilus extension *and* retraction and that altering their interfaces could affect the ability of the T4P machinery to switch between those states.

Previous work in *T. thermophilus* suggested that a dimeric complex of PilMN (two PilMs and two PilNs) forms an intermediate transmembrane platform onto which other alignment subcomplex components dock (29). The addition of PilO to the PilMN subassembly was proposed to dissociate PilN homodimers, sequestering each monomer into a PilNO heterodimer. Our data support an alternative model, in which PilN and PilO might homodimerize via their core domains (Fig. 9*C*), and simultaneously heterodimerize via their coiled coils and potentially their TMS (Fig. 9*B*) (42). This scenario could explain how untagged covalent PilN homodimers were co-purified with tagged PilO homodimers, as both constructs retain their coiled coils (Fig. 3). Alternatively, tetrameric arrangement of PilN and PilO homodimers could suggest an alternative PilNO interface on the "side" of the core homodimer interface (Fig. 9*B*); however, we have no evidence to support that idea. The PilN^{R142C} and PilO^{D175C} residues are located near the base of the modeled core interfaces and could be oriented more laterally (Fig. 9*B*) than depicted by our static models (Fig. 1), explaining why these particular residues were the only ones that successfully formed cross-linked homo- and heterodimers.

Modulation of the PilNO Core Interface by the Other Alignment Subcomplex Components—Cross-linking of Cys residues at select locations within the PilNO equivalents (GspLM) in the T2S system suggested rotation of the proteins through their TMS and periplasmic cores (34). In the T2S system, PilM orthologs interact with the single cytoplasmic motor ATPase (51–54), and more recently, interactions between PilM and the T4P motor ATPases in *P. aeruginosa* and *M. xanthus* were confirmed (40, 41). Thus, we tested whether interactions with the cytoplasmic component of the alignment subcomplex, PilM,

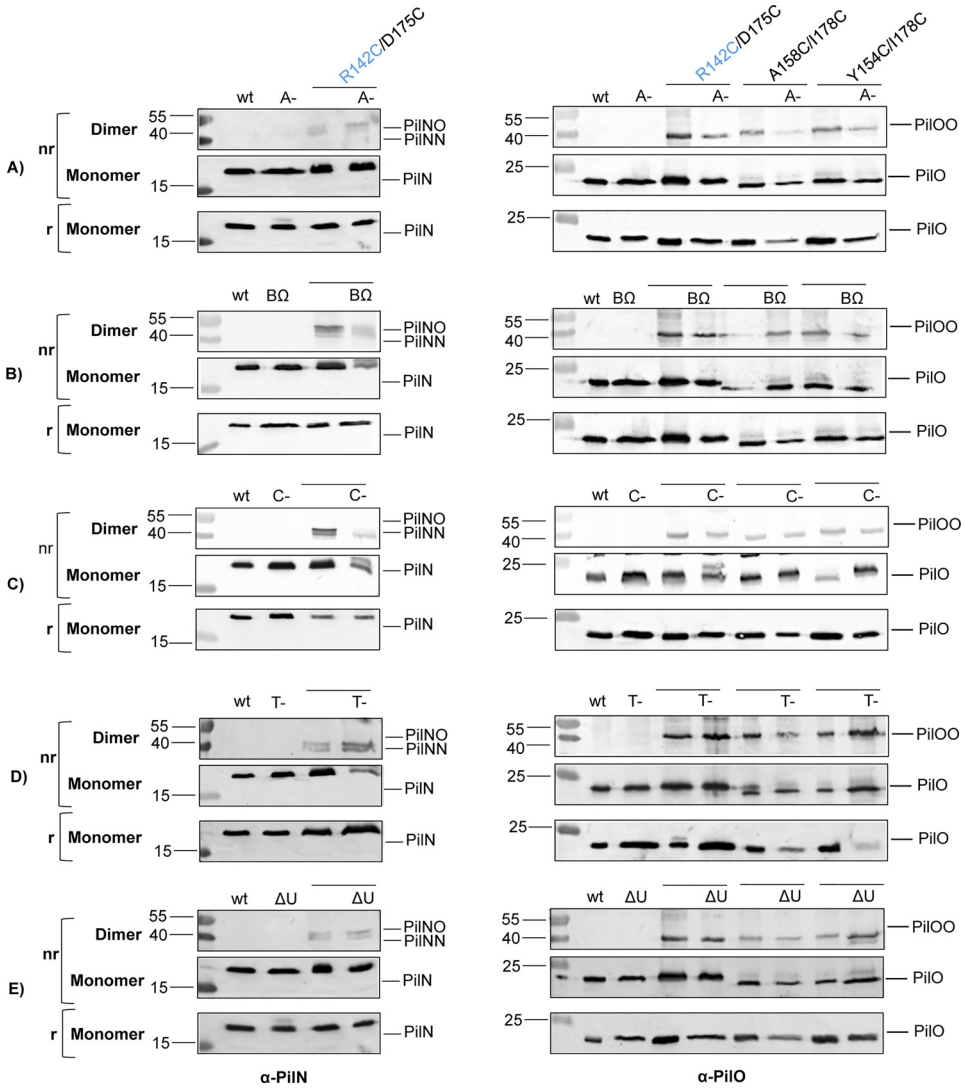

FIGURE 8. **Dimerization of PilN^{R142C}/PilO^{D175C}, PilO$^{A158C/I178C}$, and PilO$^{Y154C/I178C}$ is unaffected by loss of non-alignment subcomplex components.** Wild type (*wt*), negative controls (*A-*, *BΩ*, *C-*, *N-*, *O-*, *T-*, and *ΔU*) and Cys mutant lysates were tested for the ability of PilN and PilO to form homo- or heterodimers on non-reducing SDS-PAGE in various T4P mutant backgrounds: *(A) pilA*, *(B) pilB*, *(C) pilC*, *(D) pilT*, and *(E) pilU*. PilN (*left*) and PilO (*right*) were blotted for using protein-specific antisera. *Minus signs* indicate the gene was disrupted via an FRT insertion; Δ indicates the gene was produced by a deletion of the gene, and Ω indicates the gene was disrupted by an Ω cassette insertion. Images represent at least three independent experiments.

which is bound to the N terminus of PilN, modulated PilNO interfaces. PilN^{R142C}/PilO^{D175C} heterodimers, but not homodimers, were lost in the absence of PilM (Fig. 6, *B* and *C*), suggesting that the PilNO interface no longer adopts an orientation permissive for disulfide bond formation. New crystal structures of a *P. aeruginosa* PilM homodimer and of monomeric PilM fused to part of its binding partner, PilN(1–12), revealed that in the absence of PilN, the seven N-terminal residues of PilM (PilM(1–7)) bind in the PilN binding cleft of a second PilM monomer (41). Thus, PilM dimerizes in the absence of PilN. In this scenario, the lack of PilM-PilN interaction may favor PilN and PilO homodimer formation, whereas when PilM becomes monomeric upon binding PilN's N terminus, a corresponding shift in the position of the PilNO interfaces could induce heterodimer formation. PilM's interactions with its cytoplasmic partners, PilB, PilT, and/or PilC (41), differ depending on whether it is bound to PilN, potentially revealing a mechanism for switching between active and resting systems or between pilus assembly and disassembly. These differential interactions might similarly modulate PilNO homo- *versus* heterodimer states in the periplasm. Disruption of *pilB*, *pilT*, or *pilU* had no effect on PilN and PilO dimerization (Fig. 8, *B*, *D*, and *E*). We considered that in the absence of one ATPase (*e.g.* PilB), one of the other two (PilT or PilU) may interact with PilM, stabilizing a configuration permissive for the formation of PilNO homo- and heterodimers. However, removal of PilC, the proposed interaction partner for all three ATPases, had no effect on dimerization states (Fig. 8*C*).

The major pilin interacts with PilNOPQ in *P. aeruginosa* (19), but its specific interaction partner(s) are unknown. Transmission electron microscopy studies of *T. thermophilus* revealed a stable complex composed of soluble fragments of PilMNO-PilA (29) with PilN interacting directly with PilA. One could envision that PilN and PilO might help extract PilA from the IM during assembly, priming the base of the pilus fiber for incorporation of the next PilA subunit.

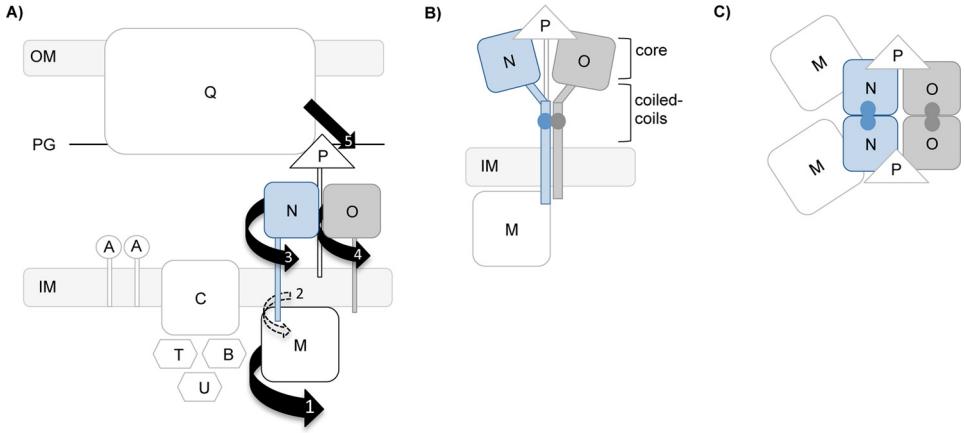

FIGURE 9. **Model of the interaction of PilN and PilO with other T4P components.** *A,* schematic of the T4P system in *P. aeruginosa* with the Pil nomenclature. Major cell compartments are labeled as follows: inner membrane (*IM*), peptidoglycan (*PG*), and outer membrane (*OM*). Specific T4P components are highlighted as follows: PilQ, the secretin; PilC, the IM platform protein; PilBTU, the three cytoplasmic ATPases; PilA, the major pilin subunit; and PilMNOP, the alignment subcomplex components. *Numbered arrows* indicate order of hypothesized movement generated from the cytoplasm outwards. *B,* T4P system schematic model showing PilN and PilO heterodimer formation mediated through the coiled coils. *C,* top-down view of PilN and PilO homodimers mediated through their core domains. Domain movement in PilM could be transduced through PilN and PilO, ultimately leading to a movement of PilP, creating a signal transduction network between the inner and outer T4P components.

However, loss of *pilA* had no effect on PilNO dimerization states (Fig. 8*A*).

In *M. xanthus,* PilQ recruits PilP, which binds PilN and PilO, and PilN binds PilM, creating a transenvelope complex (55). In *P. aeruginosa*, a similar pathway has been proposed, where PilP binds PilQ as well as PilNO but does not bind PilO homodimers (20). Here, loss of PilP prevented formation of $PilN^{R142C}$/$PilO^{D175C}$ heterodimers (Fig. 6, *D* and *E*), although loss of PilQ had no effect (Fig. 6, *F* and *G*). The core regions of PilN or PilO may homodimerize (Fig. 9*C*), and the large electrostatic difference predicted for the coiled coils of PilN and PilO (18) could promote heterodimerization (Fig. 9*B*). The unstructured N terminus of PilP could interact with the core or coiled-coil regions of PilNO heterodimers, stabilizing the interface in an orientation that allowed for disulfide bond formation.

PilN and PilO Rearrangement during "Active" and "Resting" States of the T4P System—Elegant cryoelectron tomography studies of the *M. xanthus* T4P system allowed for derivation of a "pseudo-atomic" model that implied differences between active and resting states of the machinery (49). The active state occurs during assembly or disassembly of the fiber, when a PilB or PilT ATPase is engaged at the base of the system, whereas the resting state was ATPase-free. PilM was proposed to form a ring surrounding a dimer of PilC, and expansion of the ring upon binding of PilB or PilT to PilC during the active state, accompanied by rearrangement of the density associated with PilN and PilO's coiled coils, was observed (49). Without PilM, density corresponding to PilC and the ATPases was missing (49). In our work, only PilM or PilP could modulate the PilNO core interface. We speculate that subtle reorientation of PilN and PilO may occur during the transition between resting and active or "extension" *versus* "retraction" states of the T4P system, consistent with the hypothesis that PilM may disengage from PilN (41). Although a ratcheting-type mechanism, in which PilNO conformational dynamics might contribute to the stepwise addition or removal of pilin subunits cannot yet be ruled out, our data do not support this idea.

Experimental Procedures

Strains, Media, and Growth Conditions—Bacterial strains used in this study are listed in Table 1. *E. coli* and *P. aeruginosa* were grown at 37 °C in Luria-Bertani (LB) media supplemented with antibiotics at the following final concentrations when necessary ($\mu g \cdot ml^{-1}$): ampicillin, 100; carbapenem (Cb), 200; kanamycin, 50; gentamicin (Gm), 15 for *E. coli* and 30 for *P. aeruginosa*, unless otherwise specified. Bacterial strains were stored at −80 °C in LB with 20% glycerol (v/v). Plasmids were transformed by heat shock into chemically competent cells. All constructs were verified by DNA sequencing (MOBIX, McMaster University).

Generation of Cys Mutants—Sets of double Cys mutations in PilO, as well as single Cys mutations in PilN and PilO, were chosen with reference to the $PilO_{\Delta 68}$ homodimer crystal structure Protein Data Bank code 2RJZ (18) and a $PilN_{\Delta 57}$/$PilO_{\Delta 68}$ heterodimer homology model, created by substituting the Phyre[2] generated $PilN_{\Delta 57}$ monomer in place of a PilO subunit in the PilO homodimer structure (18, 45). Distances were measured in PyMOL, and residues were selected to ensure that the distance between Cβ atoms was less than 8 Å (Fig. 1). Codons for selected Cys substitutions were introduced into either a pEX18Gm::*pilMNOP* construct (for PilNO Cys pairs) or a pEX18Gm::*pilNOP* construct (for double PilO Cys mutants) using the QuikChange site-directed mutagenesis kit (Stratagene) following the manufacturer's protocol. Mutations were verified by DNA sequencing (MOBIX).

Generation of pilN and pilO Cys Mutations onto the Chromosome of P. aeruginosa PAK—Cys-encoding chromosomal mutants of *P. aeruginosa* were generated by biparental mating with *E. coli* SM10 using a Flp-FRT (FLP recombination target) system as described previously (18). Constructs containing the desired Cys substitutions, pEX18Gm::*pilMNOP* for PilNO Cys mutants and pEX18Gm::*pilNOP* for PilO Cys mutants, were introduced into *E. coli* SM10 cells for biparental mating with PAK *pilN*::*FRT* and PAK *pilO*::*FRT,* respectively (12). The *E. coli* SM10 donor was counter-selected by plating on *Pseu-*

TABLE 1
Bacterial strains

Strain	Description	Source/Ref.
***E. coli* strains**		
DH5α	F−, φ80lacZ, M15,Δ (lacZYA-argF), U169, recA1, endA1, hsdR17 (rk−,mk+), phoAsupE44, thi-1, gyrA96, relA1, λ-	Invitrogen
Origami2 (DE3)pLysS	Δ(ara-leu)7697 ΔlacX74 ΔphoA PvuII phoR araD139 ahpC galE galK rpsL F′[lac$^+$ lacI^q pro] (DE3) gor522::Tn10 trxB pLysS (Cam^R, Str^R, Tet^R)	Novagen
SM10	thi-1, thr, leu, tonA, lacy, supE, recA, RP4-2-Tcr::Mu, Km^r; mobilizes plasmids into *P. aeruginosa* via conjugation	62
***P. aeruginosa* strains**		
PAK	Wild type	J. Boyd
Δ*pilM*	Deletion of *pilM*	17
pilN::*FRT*	FRT scar at position 124 within *pilN*	17
pilO::*FRT*	FRT scar at position 328 within *pilO*	17
pilP::*FRT*	FRT scar at position 86 within *pilP*	17
pilQ::*FRT*	FRT scar at position at 571 within *pilQ*	60
pilT::*FRT*	FRT scar at position 540 within *pilT*	47
pilA::*FRT*	FRT scar at SphI site within *pilA*	59
*pilB*Ω	*pilB* with Ω cassette insertion	61
Δ*pilU*	Deletion of *pilU*	Dr. M. Wolfgang
pilC::*FRT*	FRT scar at position 365 within *pilC*	14
PilN^{R142C}/PilO^{D175C}	*pilN* R142C and *pilO* D175C	This study
PilN^{E157C}/PilO^{A158C}	*pilN* E157C and *pilO* A158C	This study
PilN^{E132C}/PilO^{I178C}	*pilN* E132C and *pilO* I178C	This study
PilN^{R142C}/PilO^{A158C}	*pilN* R142C and *pilO* A158C	This study
PilO$^{S166C/D175C}$	*pilO* S166C, D175C	This study
PilO$^{V161C/D175C}$	*pilO* V161C, D175C	This study
PilO$^{A158C/I178C}$	*pilO* A158C, I178C	This study
PilO$^{Y154C/I178C}$	*pilO* Y154C, I178C	This study
PilN^{R142C}	*pilN* R142C	This study
PilO^{Y154C}	*pilO* Y154C	This study
PilO^{A158C}	*pilO* A158C	This study
PilO^{V161C}	*pilO* V161C	This study
PilO^{S166C}	*pilO* S166C	This study
PilO^{D175C}	*pilO* D175C	This study
PilO^{I178C}	*pilO* I178C	This study
PilN^{R142C}/PilO^{D175C} Δ*pilM*	*pilN* R142C and *pilO* D175C with deletion of *pilM*	This study
PilO$^{A158C/I178C}$ Δ*pilM*	*pilO* A158C, I178C with deletion of *pilM*	This study
PilO$^{Y154C/I178C}$ Δ*pilM*	*pilO* V154C, I178C with deletion of *pilM*	This study
PilN^{R142C}/PilO^{D175C} *pilA*::*FRT*	*pilN* R142C and *pilO* D175C with FRT insertion at SphI site within *pilA*	This study
PilO$^{A158C/I178C}$ *pilA*::*FRT*	*pilO* A158C, I178C with FRT insertion at SphI site within *pilA*	This study
PilO$^{Y154C/I178C}$ *pilA*::*FRT*	*pilO* Y154C, I178C with FRT insertion at SphI site within *pilA*	This study
PilN^{R142C}/PilO^{D175C} *pilB*Ω	*pilN* R142C and *pilO* D175C with Ω cassette insertion *pilB*	This study
PilO$^{A158C/I178C}$ *pilB*Ω	*pilO* A158C, I178C with Ω cassette insertion *pilB*	This study
PilO$^{Y154C/I178C}$ *pilB*Ω	*pilO* V154C, I178C with Ω cassette insertion *pilB*	This study
PilN^{R142C}/PilO^{D175C} *pilC*::*FRT*	*pilN* R142C and *pilO* D175C with FRT insertion at position 365 within *pilC*	This study
PilO$^{A158C/I178C}$ *pilC*::*FRT*	*pilO* A158C, I178C with FRT insertion at position 365 within *pilC*	This study
PilO$^{Y154C/I178C}$ *pilC*::*FRT*	*pilO* V154C, I178C with FRT insertion at position 365 within *pilC*	This study
PilN^{R142C}/PilO^{D175C} *pilP*::*FRT*	*pilN* R142C and *pilO* D175C with FRT insertion at position 86 within *pilP*	This study
PilO$^{A158C/I178C}$ *pilP*::*FRT*	*pilO* A158C, I178C with FRT insertion at position 86 within *pilP*	This study
PilO$^{Y154C/I178C}$ *pilP*::*FRT*	*pilO* V154C, I178C with FRT insertion at position 86 within *pilP*	This study
PilN^{R142C}/PilO^{D175C} *pilQ*::*FRT*	*pilN* R142C and *pilO* D175C with FRT insertion at position 571 within *pilQ*	This study
PilN^{R142C}/PilO^{D175C} *pilT*::*FRT*	*pilN* R142C and *pilO* D175C with FRT insertion at position 540 within *pilT*	This study
PilO$^{A158C/I178C}$ *pilT*::*FRT*	*pilO* A158C, D178C with FRT insertion at position 540 within *pilT*	This study
PilO$^{Y154C/I178C}$ *pilT*::*FRT*	*pilO* V154C, D178C with FRT insertion at position 540 within *pilT*	This study
PilN^{R142C}/PilO^{D175C} Δ*pilU*	*pilN* R142C and *pilO* D175C with deletion of *pilU*	This study
PilO$^{A158C/I178C}$ Δ*pilU*	*pilO* A158C, I178C with deletion of *pilU*	This study
PilO$^{Y154C/I178C}$ Δ*pilU*	*pilO* Y154C, I178C with deletion of *pilU*	This study

domonas isolation agar (PIA; Difco) containing Gm (100 μg·ml^{-1}). Gm-resistant *P. aeruginosa* isolates were streaked on LB-no salt sucrose plates (1% w/v bacto-tryptone, 0.5% w/v bacto-yeast extract, 5% w/v sucrose) and then incubated for 16 h at 30 °C. Select colonies were restreaked in parallel on LB and LB plates supplemented with Gm. Gm-sensitive colonies were screened by PCR using *pilN* or *pilO* primer pairs (Table 2) to confirm replacement of the original FRT-disrupted gene, and PCR products of the expected size were DNA-sequenced (MOBIX) to confirm incorporation of the desired mutations.

Preparation of Whole Cell Lysates—P. aeruginosa strains were grown on LB agar plates overnight at 37 °C. Cells were scraped from the surface and resuspended in 1× PBS (pH 7.4) to an A_{600} of 0.6. A 1-ml aliquot of cells was collected by centrifugation at 2292 × *g* for 3 min in a microcentrifuge. The cell pellet was resuspended in 100 μl of either 1× SDS-PAGE loading buffer (125 mM Tris, pH 6.8, 2% (v/v) β-ME, 20% (v/v) glycerol, 4% (w/v) SDS, and 0.001% (w/v) bromphenol blue) or 1× non-reducing SDS-PAGE loading buffer (no β-ME) and subjected to Western blotting analysis. Biological and technical replicates of all strains were performed $n \geq 3$.

Western Blotting Analysis—Samples were separated on 15% SDS-polyacrylamide gels for 1.5 h at 160 V and transferred to nitrocellulose membranes for 1 h at 225 mA. Membranes were blocked using a 5% (w/v) low fat skim milk powder in 1× PBS for 1 h at room temperature on a shaking platform, followed by incubation with protein-specific antibodies at the following dilutions: α-PilM, α-PilN, α-PilO, and α-PilP at dilutions of 1:1000 (17); α-PilB, α-PilT, and α-PilU at 1:2000, 1:500, and 1:5000, respectively (56); α-PilA at 1:5000 (57), and α-PilC at

TABLE 2
Oligonucleotide primer sequences
Fwd means forward, and Rev means reverse.

Primer name	Oligonucleotide Sequence (5′–3′)
PilA Fwd	TATATAACTCTAGAGATGAAAGCTCAAAAAGGCTTT
PilA Rev	TATTATAAGAATTCGTTACTTAGAGCAACC
PilB Fwd	TATATAACTCTAGAGATGAACGACAGCAT
PilB Rev	TATTATAAGAATTCGTTAATCCTTGGTCAC
PilC Fwd	TATATAACTCTAGAGATGGCGGACAAAGCGTTAAAAACCAG
PilC Rev	TATATATGGAATTCGTTATCCGACGACGTTGCCGAG
PilM Fwd	TATATATATCTAGAGGTGCTAGGGCTCATAAAGAAGAAAG
PilM Rev	TATTATAAGAATTCGTCAGTCGAAACTCCTCAACGCC
PilN Fwd	TATATAACTCTAGAGATGGCACGGATCAACCTTCTACCCTGG
PilN Rev	TATATATGGAATTCGTCATTTCTTGGCTCCTTGCGCAACCCC
PilO Fwd	TATATATATCTAGAGATGAGTCTGGCCAGTTCCCTG
PilO Rev	TATATATAGAATTCGTCATTTCTTCAGCCCCTTGTCG
PilP Fwd	TATATATGGAATTCGATGAGAGCCCGC
PilP Rev	TATATATAGAATTCGTCAGGAGCGTTCCTTGAGAGTC
PilT Fwd	TATATAACTCTAGAGATGGATATTACCGAGCTG
PilT Rev	TATATATAGAATTCGTCAGAAGTTTTCCGG
PilU Fwd	TATATAACTCTAGAGATGGAATTCGAAAAGCTG
PilU Rev	TATATATAGAATTCGTCAGCGGAAGCGCCG
PilN E132C Fwd	CGCCGGCGCGGCCTGCTCCAACAACCGCG
PilN E132C Rev	CGCGGTTGTTGGAGCAGGCCGCGCCGGCG
PilN R142C Fwd	CGTTTCCAATCTCATGTGCAACATGGACGCGTC
PilN R142C Rev	GACGCGTCCATGTTGCACATGAGATTGGAAACG
PilN E157C Fwd	GCCCCGACCCTGAACTGCGTCAAGGCGGTGACC
PilN E157C Rev	GGTCACCGCCTTGACGCAGTTCAGGGTCGGGGC
PilO Y154C Fwd	GTGGTCGGCGGCTGCCACGACTTGG
PilO Y154C Rev	CCAAGTCGTGGCAGCCGCCGACCAC
PilO A158C Fwd	GGCTACCACGACTTGTGCACCTTCGTCAGCGGC
PilO A158C Rev	GCCGCTGACGAAGGTGCACAAGTCGTGGTAGCC
PilO V161C Fwd	GACTTGGCGACCTTCTGCAGCGGCGTGTCCAG
PilO V161C Rev	CTGGACACGCCGCTGCAGAAGGTCGCCAAGTC
PilO S166C Fwd	GCGGCGTGTCCTGCCTGCCGCGG
PilO S166C Rev	CCGCGGCAGGCAGGACACGCCGC
PilO D175C Fwd	GGATCGTCACCCTGCATTGCTTCGAGATCAAGCCGG
PilO D175C Rev	CCGGCTTGATCTCGAAGCAATGCAGGGTGACGATCC
PilO I178C Fwd	CTGCATGACTTCGAGTGCAAGCCGGTCGCGCC
PilO I178C Rev	GGCGCGACCGGCTTGCACTCGAAGTCATGCAG

1:1000 (14). Blots were incubated in primary antibody ~16 h at 4 °C on a rocking platform. The membranes were washed twice in 1× PBS for 5 min and then incubated in goat anti-rabbit IgG-alkaline phosphatase-conjugated secondary antibody (Bio-Rad) at a dilution of 1:3000 for 1 h at room temperature. The membranes were washed twice in 1× PBS for 5 min and visualized with alkaline phosphatase developing reagent (Bio-Rad) following the manufacturer's protocol. Western blottings were performed $n \geq 3$.

Expression and Purification of $PilN_{\Delta 44}$ and $PilO_{\Delta 51}$—N-terminally truncated versions of PilN and PilO were previously cloned into the EcoRI/HindIII and NdeI/XhoI cloning sites, respectively, of a pET28a vector, creating a vector that overexpresses untagged $PilN_{\Delta 44}$ and C-terminal His_6-tagged $PilO_{\Delta 51\_His}$ (18, 20). Cys mutations were introduced into this construct using the QuikChange site-directed mutagenesis kit (Stratagene) following the manufacturer's instructions to create pET28a::$pilN_{\Delta 44}/pilO_{\Delta 51\_His}$ containing $pilN_{\Delta 44}{}^{R142C}$, $pilO_{\Delta 51}{}^{D175C}$, or a double $pilN_{\Delta 44}{}^{R142C}/pilO_{\Delta 51}{}^{D175C}$ construct. Constructs were transformed into *E. coli* Origami2 (DE3) pLysS cells and plated on LB agar plates supplemented with 50 $\mu g \cdot ml^{-1}$ kanamycin. A single colony was used to inoculate 20 ml of LB containing 50 $mg \cdot ml^{-1}$ kanamycin and incubated overnight at 37 °C with shaking. The overnight culture was used to inoculate 1 liter of fresh LB (1:100 dilution) containing antibiotic, and the cells were grown at 37 °C, with shaking, to an A_{600} of 0.6. Protein expression was induced by adding isopropyl β-D-1-thiogalactopyranoside (Sigma) to the culture at a final concentration of 1 mM. The cells were allowed to grow for 4 h at 37 °C, prior to being harvested by centrifugation (3993 × *g*, 15 min, 4 °C) in an Avanti J-26 XPI centrifuge (Beckman Coulter). Bacterial pellets were frozen at −80 °C until further use.

Bacterial pellets were thawed and resuspended in 10 ml nickel A buffer (20 mM Tris-HCl, pH 7.2, 500 mM KCl, 10 mM imidazole, 10% (v/v) glycerol) and then combined in a 50-ml screw cap tube with one complete EDTA-free protease inhibitor tablet (Roche Applied Science). Cells were lysed via sonication on ice, on setting 4, for 2 min with cycles of 10 s on and 10 s off (Sonicator 3000; Misonix). The lysates were centrifuged (11,000 × *g*, 30 min, 4 °C) in an Avanti J-26 XPI centrifuge (Beckman Coulter) to remove intact cells and other cellular debris. Pelleted material was retained for analysis by SDS-PAGE, and supernatants were filtered through 0.22-μm Acrodisc syringe filter (Pall Corp.). The lysate was purified using nickel-nitrilotriacetic acid affinity chromatography on an AKTA start FPLC (VWR Scientific). Protein lysate was flowed through a 1-ml His-Trap™ FF column (GE Healthcare) pre-equilibrated with buffer and washed with nickel A buffer and then increasing amounts of nickel B buffer (20 mM Tris-HCl, pH 7.2, 500 mM KCl, 300 mM imidazole, 10% (v/v) glycerol) in a linear gradient. The bound protein was eluted from the column in pure nickel B buffer and collected in 1-ml fractions. An aliquot of each fraction was mixed 1:1 with 2× reducing or non-reducing SDS-PAGE loading and electrophoresed on a 15% SDS-polyacrylamide gel. The gel was stained using Coomassie Blue Staining solution (0.1% Coomassie Brilliant Blue R-250,

50% (v/v) methanol, and 10% (v/v) glacial acetic acid) or developed by Western blotting using protein-specific antibodies as described above.

Twitching Motility Assays—Twitching assays were performed as described previously (5, 47, 48, 58). Briefly, single colonies were stab inoculated to the bottom of a 1% LB agar plate. The plates were incubated for 36 h at 37 °C. Postincubation, the agar was carefully removed and the adherent bacteria stained with 1% (w/v) crystal violet dye, followed by washing with tap water to remove unbound dye. Twitching zone areas were measured using ImageJ software (National Institutes of Health). Statistical significance of differences compared with wild type was determined using Student's *t* test. All experiments were performed in triplicate with at least three independent replicates.

Sheared Surface Protein Preparation—Surface pili and flagella were analyzed as described previously (58) with the following modifications. *P. aeruginosa* strains of interest were streaked in a grid-like pattern on large LB 1.5% agar plates and incubated at 37 °C for ~16 h. The cells were scraped from the plates with glass coverslips and resuspended in 4.5 ml of 1× PBS. Centrifugation of the cells was performed in 1.5-ml Eppendorf tubes at 11,688 × *g*. Cell pellets were resuspended in 150 μl of 1× SDS sample buffer (125 mM Tris, pH 6.8, 2% (v/v) β-ME, 20% (v/v) glycerol, 4% (w/v) SDS, and 0.001% (w/v) bromphenol blue) and visualized on a 15% SDS-polyacrylamide gel by staining with Coomassie Blue staining solution.

In Vivo Disulfide Cross-linking Analysis—Spontaneous disulfide bond formation between PilN and PilO Cys mutants was assessed in bacteria grown on solid media. Whole cell lysates of the various strains resuspended in reducing or non-reducing SDS-PAGE buffer were boiled for 10 min to lyse cells, electrophoresed on a 15% SDS-polyacrylamide gel, and subjected to Western blotting with protein-specific antibodies for PilN and PilO as described previously.

Generation of PilN and PilO Cys Pairs in Various T4P Component Mutant Backgrounds—To test the contributions of other T4P proteins to dimer formation, select Cys mutants were generated in previously generated T4P mutant backgrounds (Table 1). To create strains with Cys substitutions and devoid of PilM, a construct composed of 700 bp up- and downstream of the *pilM* gene (Δ*pilM*) was subcloned into pEX18Gm using XbaI/EcoRI. The resulting suicide construct was transformed into *E. coli* SM10 and transferred to *P. aeruginosa* PAK strains already containing $pilN^{R142C}/pilO^{D175C}$, $pilO^{A158C/I178C}$, or $pilO^{Y154C/I178C}$ by biparental mating, and mutants were selected as described above.

To make Cys mutant strains lacking PilA, PilC, PilQ, or PilT, we used previously engineered suicide constructs for *pilA*::FRT (59), *pilC*::FRT (14), *pilQ*::FRT (60), and *pilT*::FRT (47) mutants. These constructs were introduced into the *P. aeruginosa* PAK $PilN^{R142C}/PilO^{D175C}$, $PilO^{A158C/I178C}$, or $PilO^{Y154C/I178C}$ backgrounds, with the exception of *pilQ*::FRT, which was only introduced into the $PilN^{R142C}/PilO^{D175C}$ background. Briefly, a suicide vector containing the target gene (*pilA, pilC, pilQ,* or *pilT*) disrupted by a gentamicin resistance cassette flanked by FRT sites (pEX18Ap *pilA*::GmFRT, pEX18Ap *pilC*::GmFRT, pEX18Ap *pilQ*::GmFRT, or pEX18Ap *pilT*::GmFRT, respectively) (22) were introduced into chemically competent *E. coli* SM10 cells. The constructs were transferred to *P. aeruginosa* PAK strains containing $pilN^{R142C}/pilO^{D175C}$, $pilO^{A158C/I178C}$, or $pilO^{Y154C/I178C}$ by biparental mating as described above. After overnight incubation on sucrose plates, select colonies were plated in parallel on LB plates supplemented with either Cb or Gm, and Gm-resistant, Cb-sensitive colonies were selected. The integrated Gm cassette was removed by conjugally transferring the Flp-expressing pFLP2 from *E. coli* SM10 into *P. aeruginosa* as described previously (18). *E. coli* SM10 was counter-selected by plating on *Pseudomonas* isolation agar (Difco) containing Cb. pFLP2 was cured by streaking Cb-resistant isolates on LB-no salt plates containing 5% (w/v) sucrose and incubating for 16 h at 30 °C. Select colonies were streaked in parallel on LB plates, LB plus Cb, and LB plus Gm plates. Cb- and Gm-sensitive colonies were selected, and the *pilA*::FRT, *pilC*::FRT, *pilQ*::FRT, and *pilT*::FRT mutations were confirmed by PCR and DNA sequencing using the primers listed in Table 2.

In some cases, we started with various *P. aeruginosa* PAK mutant backgrounds, *pilB*Ω (61), *pilP*::FRT (17), and Δ*pilU* (gift of Dr. Matthew Wolfgang), and introduced suicide vectors containing the desired PilN and PilO Cys pairs (as described above). After selection for Gm-sensitive colonies, we screened for correct incorporation of PilN and PilO Cys pairs through PCR using *pilN* or *pilO* primer pairs (Table 2) and mutations were confirmed by DNA sequencing (MOBIX).

Author Contributions—T. L. L., D. H. Y., L. L. B., and P. L. H. designed the study and developed the methodology. T. L. L. and D. H. Y. created all Cys mutant strain variants. Experiments were performed by T. L. L. T. L. L., L. L. B., and P. L. H. wrote and edited the manuscript.

References

1. Bradley, D. E. (1980) A function of *Pseudomonas aeruginosa* PAO polar pili: twitching motility. *Can. J. Microbiol.* **26,** 146–154
2. Burrows, L. L. (2005) Weapons of mass retraction. *Mol. Microbiol.* **57,** 878–888
3. Burrows, L. L. (2012) *Pseudomonas aeruginosa* twitching motility: type IV pili in action. *Annu. Rev. Microbiol.* **66,** 493–520
4. Leighton, T. L., Buensuceso, R., Howell, P. L., and Burrows, L. L. (2015) Biogenesis of *Pseudomonas aeruginosa* type IV pili and regulation of their function. *Environ. Microbiol.* **17,** 4148–4163
5. Mattick, J. S. (2002) Type IV pili and twitching motility. *Annu. Rev. Microbiol.* **56,** 289–314
6. Pelicic, V. (2008) Type IV pili: e pluribus unum? *Mol. Microbiol.* **68,** 827–837
7. Strom, M. S., and Lory, S. (1993) Structure-function and biogenesis of the type IV pili. *Annu. Rev. Microbiol.* **47,** 565–596
8. Burkhardt, J., Vonck, J., and Averhoff, B. (2011) Structure and function of PilQ, a secretin of the DNA transporter from the thermophilic bacterium *Thermus thermophilus* HB27. *J. Biol. Chem.* **286,** 9977–9984
9. Collins, R. F., Davidsen, L., Derrick, J. P., Ford, R. C., and Tønjum, T. (2001) Analysis of the PilQ secretin from *Neisseria meningitidis* by transmission electron microscopy reveals a dodecameric quaternary structure. *J. Bacteriol.* **183,** 3825–3832
10. Collins, R. F., Ford, R. C., Kitmitto, A., Olsen, R. O., Tønjum, T., and Derrick, J. P. (2003) Three-dimensional structure of the *Neisseria meningitidis* secretin PilQ determined from negative-stain transmission electron microscopy. *J. Bacteriol.* **185,** 2611–2617
11. Koo, J., Burrows, L. L., and Howell, P. L. (2012) Decoding the roles of pilotins and accessory proteins in secretin escort services. *FEMS Microbiol. Lett.* **328,** 1–12

12. Koo, J., Tammam, S., Ku, S. Y., Sampaleanu, L. M., Burrows, L. L., and Howell, P. L. (2008) PilF is an outer membrane lipoprotein required for multimerization and localization of the *Pseudomonas aeruginosa* type IV pilus secretin. *J. Bacteriol.* **190,** 6961–6969
13. Chiang, P., Habash, M., and Burrows, L. L. (2005) Disparate subcellular localization patterns of *Pseudomonas aeruginosa* type IV pilus ATPases involved in twitching motility. *J. Bacteriol.* **187,** 829–839
14. Takhar, H. K., Kemp, K., Kim, M., Howell, P. L., and Burrows, L. L. (2013) The platform protein is essential for type IV pilus biogenesis. *J. Biol. Chem.* **288,** 9721–9728
15. Nguyen, Y., Jackson, S. G., Aidoo, F., Junop, M., and Burrows, L. L. (2010) Structural characterization of novel *Pseudomonas aeruginosa* type IV pilins. *J. Mol. Biol.* **395,** 491–503
16. Nguyen, Y., Sugiman-Marangos, S., Harvey, H., Bell, S. D., Charlton, C. L., Junop, M. S., and Burrows, L. L. (2015) *Pseudomonas aeruginosa* minor pilins prime type IVa pilus assembly and promote surface display of the PilY1 adhesin. *J. Biol. Chem.* **290,** 601–611
17. Ayers, M., Sampaleanu, L. M., Tammam, S., Koo, J., Harvey, H., Howell, P. L., and Burrows, L. L. (2009) PilM/N/O/P proteins form an inner membrane complex that affects the stability of the *Pseudomonas aeruginosa* type IV pilus secretin. *J. Mol. Biol.* **394,** 128–142
18. Sampaleanu, L. M., Bonanno, J. B., Ayers, M., Koo, J., Tammam, S., Burley, S. K., Almo, S. C., Burrows, L. L., and Howell, P. L. (2009) Periplasmic domains of *Pseudomonas aeruginosa* PilN and PilO form a stable heterodimeric complex. *J. Mol. Biol.* **394,** 143–159
19. Tammam, S., Sampaleanu, L. M., Koo, J., Manoharan, K., Daubaras, M., Burrows, L. L., and Howell, P. L. (2013) PilMNOPQ from the *Pseudomonas aeruginosa* type IV pilus system form a transenvelope protein interaction network that interacts with PilA. *J. Bacteriol.* **195,** 2126–2135
20. Tammam, S., Sampaleanu, L. M., Koo, J., Sundaram, P., Ayers, M., Chong, P. A., Forman-Kay, J. D., Burrows, L. L., and Howell, P. L. (2011) Characterization of the PilN, PilO and PilP type IVa pilus subcomplex. *Mol. Microbiol.* **82,** 1496–1514
21. Balasingham, S. V., Collins, R. F., Assalkhou, R., Homberset, H., Frye, S. A., Derrick, J. P., and Tønjum, T. (2007) Interactions between the lipoprotein PilP and the secretin PilQ in *Neisseria meningitidis*. *J. Bacteriol.* **189,** 5716–5727
22. Bose, N., Payne, S. M., and Taylor, R. K. (2002) Type 4 pilus biogenesis and type II-mediated protein secretion by *Vibrio cholerae* occur independently of the TonB-facilitated proton motive force. *J. Bacteriol.* **184,** 2305–2309
23. Ayers, M., Howell, P. L., and Burrows, L. L. (2010) Architecture of the type II secretion and type IV pilus machineries. *Future Microbiol.* **5,** 1203–1218
24. Douzi, B., Filloux, A., and Voulhoux, R. (2012) On the path to uncover the bacterial type II secretion system. *Philos. Trans. R. Soc. Lond. B Biol. Sci.* **367,** 1059–1072
25. Durand, E., Bernadac, A., Ball, G., Lazdunski, A., Sturgis, J. N., and Filloux, A. (2003) Type II protein secretion in *Pseudomonas aeruginosa*: the pseudopilus is a multifibrillar and adhesive structure. *J. Bacteriol.* **185,** 2749–2758
26. Abendroth, J., Bagdasarian, M., Sandkvist, M., and Hol, W. G. (2004) The structure of the cytoplasmic domain of EpsL, an inner membrane component of the type II secretion system of *Vibrio cholerae*: an unusual member of the actin-like ATPase superfamily. *J. Mol. Biol.* **344,** 619–633
27. Abendroth, J., Kreger, A. C., and Hol, W. G. (2009) The dimer formed by the periplasmic domain of EpsL from the type 2 secretion system of *Vibrio parahaemolyticus*. *J. Struct. Biol.* **168,** 313–322
28. Abendroth, J., Rice, A. E., McLuskey, K., Bagdasarian, M., and Hol, W. G. (2004) The crystal structure of the periplasmic domain of the type II secretion system protein EpsM from *Vibrio cholerae*: the simplest version of the ferredoxin fold. *J. Mol. Biol.* **338,** 585–596
29. Karuppiah, V., Collins, R. F., Thistlethwaite, A., Gao, Y., and Derrick, J. P. (2013) Structure and assembly of an inner membrane platform for initiation of type IV pilus biogenesis. *Proc. Natl. Acad. Sci. U.S.A.* **110,** E4638–E4647
30. Karuppiah, V., and Derrick, J. P. (2011) Structure of the PilM-PilN inner membrane type IV pilus biogenesis complex from *Thermus thermophilus*. *J. Biol. Chem.* **286,** 24434–24442
31. Py, B., Loiseau, L., and Barras, F. (2001) An inner membrane platform in the type II secretion machinery of Gram-negative bacteria. *EMBO Rep.* **2,** 244–248
32. Sandkvist, M., Hough, L. P., Bagdasarian, M. M., and Bagdasarian, M. (1999) Direct interaction of the EpsL and EpsM proteins of the general secretion apparatus in *Vibrio cholerae*. *J. Bacteriol.* **181,** 3129–3135
33. Robert, V., Hayes, F., Lazdunski, A., and Michel, G. P. (2002) Identification of XcpZ domains required for assembly of the secreton of *Pseudomonas aeruginosa*. *J. Bacteriol.* **184,** 1779–1782
34. Lallemand, M., Login, F. H., Guschinskaya, N., Pineau, C., Effantin, G., Robert, X., and Shevchik, V. E. (2013) Dynamic interplay between the periplasmic and transmembrane domains of GspL and GspM in the type II secretion system. *PLoS One* **8,** e79562
35. Winston, S. E., Mehan, R., and Falke, J. J. (2005) Evidence that the adaptation region of the aspartate receptor is a dynamic four-helix bundle: cysteine and disulfide scanning studies. *Biochemistry* **44,** 12655–12666
36. Seeger, M. A., von Ballmoos, C., Eicher, T., Brandstätter, L., Verrey, F., Diederichs, K., and Pos, K. M. (2008) Engineered disulfide bonds support the functional rotation mechanism of multidrug efflux pump AcrB. *Nat. Struct. Mol. Biol.* **15,** 199–205
37. Bass, R. B., Butler, S. L., Chervitz, S. A., Gloor, S. L., and Falke, J. J. (2007) Use of site-directed cysteine and disulfide chemistry to probe protein structure and dynamics: applications to soluble and transmembrane receptors of bacterial chemotaxis. *Methods Enzymol.* **423,** 25–51
38. Arts, J., de Groot, A., Ball, G., Durand, E., El Khattabi, M., Filloux, A., Tommassen, J., and Koster, M. (2007) Interaction domains in the *Pseudomonas aeruginosa* type II secretory apparatus component XcpS (GspF). *Microbiology* **153,** 1582–1592
39. Robert, V., Filloux, A., and Michel, G. P. (2005) Subcomplexes from the Xcp secretion system of *Pseudomonas aeruginosa*. *FEMS Microbiol. Lett.* **252,** 43–50
40. Bischof, L. F., Friedrich, C., Harms, A., Søgaard-Andersen, L., and van der Does, C. (2016) The type IV pilus assembly ATPase PilB of *Myxococcus xanthus* interacts with the inner membrane platform protein PilC and the nucleotide binding protein PilM. *J. Biol. Chem.* **291,** 6946–6957
41. McCallum, M., Tammam, S., Little, D. J., Robinson, H., Koo, J., Shah, M., Calmettes, C., Moraes, T. F., Burrows, L. L., and Howell, P. L. (2016) PilN binding modulates the structure and binding partners of the *Pseudomonas aeruginosa* type IVa pilus protein PilM. *J. Biol. Chem.* **291,** 11003–11015
42. Leighton, T. L., Dayalani, N., Sampaleanu, L. M., Howell, P. L., and Burrows, L. L. (2015) A novel role for PilNO in type IV pilus retraction revealed by alignment subcomplex mutations. *J. Bacteriol.* **197,** 2229–2238
43. Careaga, C. L., and Falke, J. J. (1992) Thermal motions of surface α-helices in the D-galactose chemosensory receptor. Detection by disulfide trapping. *J. Mol. Biol.* **226,** 1219–1235
44. Careaga, C. L., and Falke, J. J. (1992) Structure and dynamics of *Escherichia coli* chemosensory receptors. Engineered sulfhydryl studies. *Biophys. J.* **62,** 209–216
45. Kelley, L. A., and Sternberg, M. J. (2009) Protein structure prediction on the Web: a case study using the Phyre server. *Nat. Protoc.* **4,** 363–371
46. Wolfgang, M., Lauer, P., Park, H. S., Brossay, L., Hébert, J., and Koomey, M. (1998) PilT mutations lead to simultaneous defects in competence for natural transformation and twitching motility in piliated *Neisseria gonorrhoeae*. *Mol. Microbiol.* **29,** 321–330
47. Whitchurch, C. B., Hobbs, M., Livingston, S. P., Krishnapillai, V., and Mattick, J. S. (1991) Characterisation of a *Pseudomonas aeruginosa* twitching motility gene and evidence for a specialised protein export system widespread in eubacteria. *Gene* **101,** 33–44
48. Whitchurch, C. B., and Mattick, J. S. (1994) Characterization of a gene, *pilU*, required for twitching motility but not phage sensitivity in *Pseudomonas aeruginosa*. *Mol. Microbiol.* **13,** 1079–1091
49. Chang, Y. W., Rettberg, L. A., Treuner-Lange, A., Iwasa, J., Søgaard-Andersen, L., and Jensen, G. J. (2016) Architecture of the type IVa pilus machine. *Science* **351,** aad2001
50. Wang, X., Pineau, C., Gu, S., Guschinskaya, N., Pickersgill, R. W., and Shevchik, V. E. (2012) Cysteine scanning mutagenesis and disulfide mapping analysis of arrangement of GspC and GspD protomers within the type 2 secretion system. *J. Biol. Chem.* **287,** 19082–19093

51. Py, B., Loiseau, L., and Barras, F. (1999) Assembly of the type II secretion machinery of *Erwinia chrysanthemi*: direct interaction and associated conformational change between OutE, the putative ATP-binding component and the membrane protein OutL. *J. Mol. Biol.* **289,** 659–670
52. Sandkvist, M., Bagdasarian, M., Howard, S. P., and DiRita, V. J. (1995) Interaction between the autokinase EpsE and EpsL in the cytoplasmic membrane is required for extracellular secretion in *Vibrio cholerae*. *EMBO J.* **14,** 1664–1673
53. Gray, M. D., Bagdasarian, M., Hol, W. G., and Sandkvist, M. (2011) *In vivo* cross-linking of EpsG to EpsL suggests a role for EpsL as an ATPase-pseudopilin coupling protein in the type II secretion system of *Vibrio cholerae*. *Mol. Microbiol.* **79,** 786–798
54. Yamagata, A., Milgotina, E., Scanlon, K., Craig, L., Tainer, J. A., and Donnenberg, M. S. (2012) Structure of an essential type IV pilus biogenesis protein provides insights into pilus and type II secretion systems. *J. Mol. Biol.* **419,** 110–124
55. Friedrich, C., Bulyha, I., and Søgaard-Andersen, L. (2014) Outside-in assembly pathway of the type IV pilus system in *Myxococcus xanthus*. *J. Bacteriol.* **196,** 378–390
56. Chiang, P., Sampaleanu, L. M., Ayers, M., Pahuta, M., Howell, P. L., and Burrows, L. L. (2008) Functional role of conserved residues in the characteristic secretion NTPase motifs of the *Pseudomonas aeruginosa* type IV pilus motor proteins PilB, PilT and PilU. *Microbiology* **154,** 114–126
57. Harvey, H., Habash, M., Aidoo, F., and Burrows, L. L. (2009) Single-residue changes in the C-terminal disulfide-bonded loop of the *Pseudomonas aeruginosa* type IV pilin influence pilus assembly and twitching motility. *J. Bacteriol.* **191,** 6513–6524
58. Kus, J. V., Tullis, E., Cvitkovitch, D. G., and Burrows, L. L. (2004) Significant differences in type IV pilin allele distribution among *Pseudomonas aeruginosa* isolates from cystic fibrosis (CF) versus non-CF patients. *Microbiology* **150,** 1315–1326
59. Kus, J. V., Kelly, J., Tessier, L., Harvey, H., Cvitkovitch, D. G., and Burrows, L. L. (2008) Modification of *Pseudomonas aeruginosa* Pa5196 type IV pilins at multiple sites with D-Araf by a novel GT-C family arabinosyltransferase, TfpW. *J. Bacteriol.* **190,** 7464–7478
60. Koo, J., Tang, T., Harvey, H., Tammam, S., Sampaleanu, L., Burrows, L. L., and Howell, P. L. (2013) Functional mapping of PilF and PilQ in the *Pseudomonas aeruginosa* type IV pilus system. *Biochemistry* **52,** 2914–2923
61. Nunn, D., Bergman, S., and Lory, S. (1990) Products of three accessory genes, pilB, *pilC*, and *pilD*, are required for biogenesis of *Pseudomonas aeruginosa* pili. *J. Bacteriol.* **172,** 2911–2919
62. Simon, V., and Schumann, W. (1987) *In vivo* formation of gene fusions in *Pseudomonas putida* and construction of versatile broad-host-range vectors for direct subcloning of Mu d1 and Mu d2 fusions. *Appl. Environ. Microbiol.* **53,** 1649–1654